THE JOURNAL
OF
CHEMICAL PHYSICS

VOLUME 2 JUNE, 1934 NUMBER 6

The Infrared Absorption of Water from 2.5μ to 6.5μ

E. K. PLYLER AND C. J. CRAVEN, *Department of Physics, University of North Carolina*
(Received February 26, 1934)

A study has been made of the infrared absorption bands of water from 2.5μ to 6.5μ and new bands have been found at 3.30μ, 5.56μ and 5.83μ. The band at 4.7μ showed an irregular envelope and may contain several components. The 3μ band showed a shift with thickness and is probably made up of four components. The change in position of the maximum in the 3μ region with thickness is explained as due to difference in sharpness of the components which constitute the band. The band at 6.15μ did not show the corresponding shift with thickness.

MANY studies have been made on the absorption of water, but only in recent years have studies been made with instruments of moderate or high resolution. Practically all of the recent work[1, 2] has been concentrated in the near infrared and has not included the bands at 3μ, 4.7μ and 6.1μ. All the absorption bands of water were once thought to be harmonics of the intense band at 6.1μ, but newly discovered bands at 1.74μ, 1.79μ, 2.79μ, 2.90μ and 3.14μ indicate that the absorption of water is more complex.

The present work was undertaken to extend the study of water through the strong band in the region of 6.1μ. In starting a study of solutions in this region it was found of importance to know the position and percent absorption of the bands of water.

A Hilger infrared spectrometer with a fluorite prism was used as the resolving instrument and a thermocouple made by Dr. J. D. Hardy was used to detect the radiation. The spectrometer and other equipment were the same as used in previous work. Cells with fluorite windows were used to hold the water, and the water layer varied in thickness from 0.1 mm to 0.001 mm. The cells were made by putting a drop of water between the plates and pressing to the desired thickness. The plates were sealed around the edges with wax which prevented vaporization and also held the cell to a constant thickness.

The 3μ region was studied at the outset and it was found that the region of maximum absorption was a function of the cell thickness. Then the series of absorption curves which are shown in Fig. 1 was obtained by using cells of different thicknesses. It is seen that the position of maximum absorption occurs at 3.18μ for the thickest cell which transmitted only 5 percent of the radiant energy, and at about 2.94μ for the thinnest cell which transmitted 80 percent of the radiant energy. With still thinner cells this maximum probably would be around 2.91μ, which is the position given by Raman spectra.[3] In Fig. 2 are shown more accurate results obtained when 0.1 mm slits were used and the readings were taken at intervals of 0.02μ. The third curve shows bands at 3.18μ and 3.30μ.

[1] J. R. Collins, Phys. Rev. **20**, 486 (1922).
[2] J. W. Ellis, Phys. Rev. **38**, 693 (1931).
[3] E. L. Kinsey, Phys. Rev. **34**, 541 (1929).

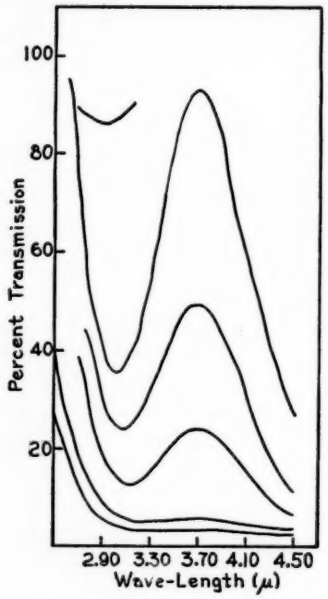

FIG. 1. The variation in transmission of water in the 3μ region due to change in thickness.

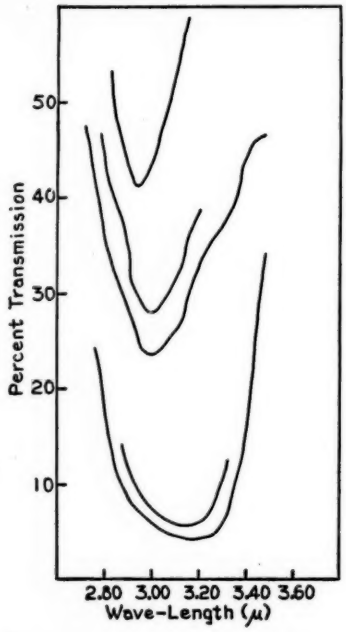

FIG. 2. The variation in transmission of water in the 3μ region due to change in thickness, with higher resolution.

The band at 3.14μ in Raman spectra may be the one shown here at 3.18μ, but the one at 3.30μ has not been previously observed.

The shift in the maximum of absorption of a band is found to be caused by temperature changes, and a change in position due to thickness is found when a weak band is located close by an intense band. The shift of the 3μ water band is not due to either of these effects, but may be the result of its complex nature. From the work of Kinsey[3] bands have been found at 2.79μ, 2.90μ and 3.14μ, and in the present work bands have been observed at 3.18μ and 3.30μ. These four overlapping bands produced the absorption which is called the 3μ water band. The intensity of the maximum absorption in a sharp band will increase more rapidly than in a broad one. If we assume that the bands which overlap in the 3μ region vary in sharpness, which seems probable as they arise from different types of vibration, the position of maximum absorption in the resultant band will be a function of cell thickness. Collins[4] has observed that the near infrared bands of water shift in position and intensity as the temperature is changed. He interpreted these changes as due to a change in the number of di-, and trihydrol molecules. While this effect may be due to the change in the groupings of water molecules, yet the same effect could be produced if these bands are made up of two or more components of different sharpness which vary in intensity with the temperature. According to the classification of Ellis[2] the bands at 1.96μ, 1.45μ, 1.18μ and 0.98μ are all double, and a shift (may be) produced by a change in thickness or temperature.

When cells with thicknesses from 0.01 mm to 0.001 mm are used, no bands appear in the region from 3.5μ to 6μ. With a cell of about 0.06 mm thickness bands were observed as shown in Fig. 3. Besides the band at 4.70μ, two other bands, which previously have not been observed, have been found at 5.56μ and 5.83μ. In thick cells the band at 5.5μ appears more intense, but with cells of decreasing thickness the 5.83μ band becomes more intense. It was also noticed that the positions of these bands varied with cell thickness. These effects are probably due to these weak bands being on the side on an intense band. The wave-lengths given for these bands are taken from the upper curve. These bands have low intensity in comparison to that

[4] J. R. Collins, Phys. Rev. 26, 771 (1925).

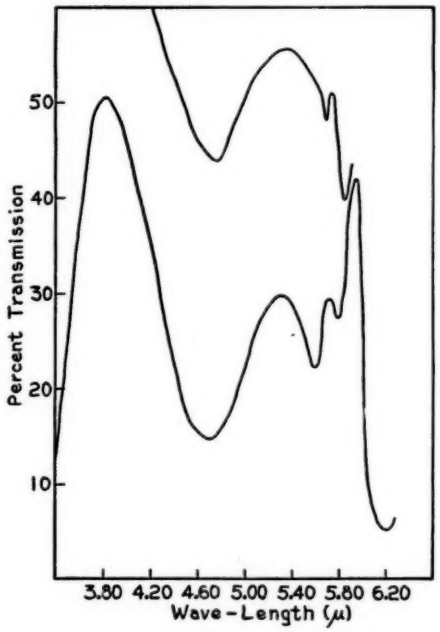

FIG. 3. The transmission of water from 3.40μ to 6.20μ for two cell thicknesses.

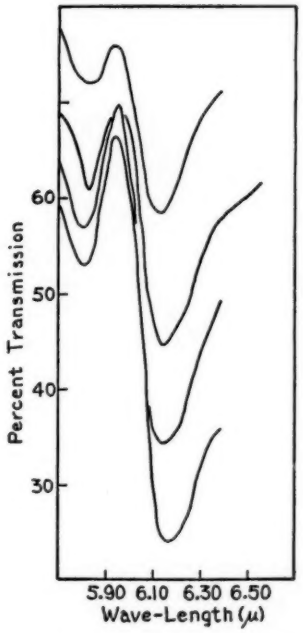

FIG. 4. The transmission of water from 5.70μ to 6.50μ for four cell thicknesses.

in the 6μ region and may arise due to differences in other frequencies or, at least, one of them may be a second harmonic of a long wave-length band. Such a band has been proposed by Ellis to account for the presence of certain short wave-length bands. The 4.7μ band seems to become irregular with thin cells and to be made up of several bands. The different maxima could never be clearly found but it will be noticed in the upper curve of Fig. 3 that there is a slight shift of the band and that an irregularity appears on the side of the band.

The absorption in the region of 6μ was studied as a function of the cell thickness, but no appreciable shift in the band was observed. In Fig. 4 are shown the results obtained with cells from 0.001 to 0.1 mm in thickness. The lowest curve in Fig. 3 or in Fig. 4 shows the maxima at 6.18μ, while all other curves give 6.15μ. This makes it seem probable that the absorption in the 6.15μ region of water is due to a single band.

It is expected to continue this work into the longer wave-length region. It can then be seen if there exists another fundamental band for water in the region from 16μ to 20μ. Until the longer wave-length region is studied, it is impossible to make a complete classification of the vibrational bands in water.

The Infrared Absorption of Acid Solutions

E. K. PLYLER AND E. S. BARR, *Department of Physics, University of North Carolina*

(Received February 26, 1934)

A study has been made of the absorption of aqueous solutions of HCl, HF, HBr, H_2SO_4, HNO_3, NaCl and NaBr in the region from 1.7μ to 6.5μ. Also HCOOH, C_6H_5COOH have been studied from 5μ to 6.5μ. No absorption bands were found for HCl and HBr in the regions of 3.5μ and 3.8μ, respectively, where there are strong bands in the gaseous state. All of the acid solutions showed a strong band at about 5.5μ. The position of this band varied slightly with the solute and the sharpness of the band was different for each acid. Another band was found at 2.40μ for the solutes. The 5.5μ band is explained as due to the undissociated molecule attached to a water molecule and the 2.40μ band as due to the same effect or to a hydrogen ion attached to a water molecule.

CONSIDERABLE work has been done on the absorption of solutions in the near infrared by H. C. Jones and his co-workers.[1] These researches did not extend beyond 1.5μ and left a large region of the infrared unexplored. Also very little attention was given to the study of inorganic acids and bases. In many cases the bands were due to harmonics and combinations and thus were difficult to interpret. The work of Collins[2] to 2.2μ on the absorption of 16 inorganic compounds in solution showed that the absorption of water was influenced by the presence of the solute. Collins was not interested in finding bands due to solutes, but he showed that the hydroxides had bands in the regions of 0.96μ, 1.1μ and 1.27μ. Grantham[3] had previously shown than NaOH, KOH, LiOH and CsOH had a band at 2.29μ and NH_4OH had a band at 2.20μ. In view of the agreement in position of this absorption band for the various hydroxides, Grantham concluded that it was due to the dissociated OH ion.

All ions, except those which are monatomic, should have characteristic absorption bands; and a monatomic ion, if attached to a water molecule, may also produce an absorption band. Due to the difficulty in interpreting overlapping bands in the shorter wave-length region, it was felt that further and more definite information could be best obtained by work in the longer wave-length regions. For this reason, the present work has been concentrated in the region from 1.7μ to 6.5μ.

A Hilger infrared spectrometer with fluorite prism was used for resolving the spectra and a thermopile with galvanometer was used for detecting the radiation. The galvanometer was used in connection with a Moll thermorelay with a subsidiary galvanometer, which greatly increased the deflections. The other arrangements were of the usual type.

The greatest difficulty was found in determining the thickness of cell to bring out the bands properly. Because of the intense absorption of water at 3μ and 6μ, extremely thin layers of the solution were used. Below 2.8μ the cells were made of two very thin glass plates, 0.1 mm apart. For the longer wave-lengths either mica or fluorite plates were used. For some of the thicker cells thin mica washers were satisfactory, but a great portion of this investigation was done with thicknesses of solution from 0.001 mm to 0.01 mm. Since washers are impractical for such cells, it was found necessary to make cells of varying thicknesses and test each one until a satisfactory thickness was obtained. The general procedure was to take one of the plates, put a drop or so of the solution on it, place the other plate upon it, and then move the plates one upon the other until the liquid was evenly distributed and the layer sufficiently thin. The plates were then sealed. The plates used had an area of some 4 sq. cm. These extremely thin cells were necessary, for otherwise the intense

[1] Jones, *Absorption Spectra of Solutions*, Carnegie Inst. of Washington, Publication Number 210.

[2] J. R. Collins, Phys. Rev. **20**, 486 (1922).

[3] G. E. Grantham, Phys. Rev. **18**, 339 (1921).

absorption of water at 3μ would have masked any absorption due to the solute.

The first work in this investigation was done in the region between 1.6μ and 2.8μ. In Fig. 1 are shown the transmission curves for H_2O, 36 percent HCl, 65 percent HNO_3, 32 percent HNO_3, and in Fig. 2, those of saturated solution NaCl, 48 percent HBr, 48 percent H_2SO_4, 96 percent H_2SO_4. The cell thickness was very nearly the same in all cases, as may be known from their having approximately the same transmission at 1.6μ. From these curves it can clearly be seen that there is a marked effect in the region of about 2.40μ due to the presence of various acids. In order to determine whether these bands were due in any sense to the negative ion, curves were obtained for NaCl and NaBr in saturated solutions at 23°C. If the absorption in the curves for the solutions of HCl or HBr was due to the negative ion attached to a water molecule, the band at 2.40μ should also appear in curves for these salts. An inspection of Fig. 2 will show that no such absorption has been observed in NaCl. NaBr likewise failed to show any absorption. If there is any modification of the 2μ absorption band of water at all, due to the presence of the solutes, it is not to any great extent. The study of the modification of water bands was not the purpose of this investigation and a careful study of the point has not been made. The percentage transmissions of the solutions as compared with that of water is shown in Fig. 3. All the acids studied give a strong band in the region of 2.40μ, which is attributed to either an undissociated acid molecule or a hydrogen ion attached to a water molecule. The curves have in general the same shape, except that for 65 percent HNO_3. The distortion of this band may be due to the NO_3 ion. It should also be kept in mind that when the percent transmission of a solution is plotted against the transmission of water, small errors in the original data are greatly magnified. In the region from 2.7μ to 4.9μ the transmission of the solutions was practically identical with that of water and, as in the case of the 2μ water band, there was no appreciable modification of the 3μ band due to the presence of the solutes.

HCl in the gaseous state has an intense absorption band at about 3.5μ. This region was carefully studied in an effort to determine if this band were present in solution. The band was not found, and this non-appearance is taken as an indication that, when in an aqueous solution, there can be only a small percent, if any, of the HCl molecules in a state similar to that of those

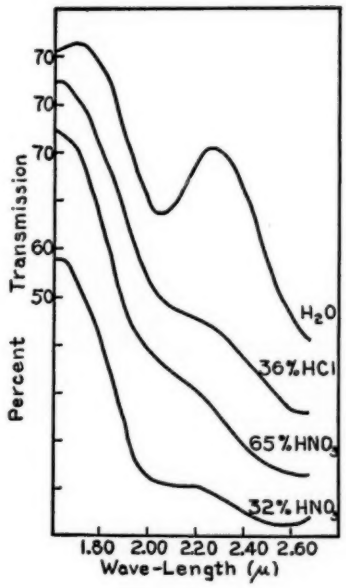

FIG. 1. Percent transmission of water, 36 percent HCl, 65 percent HNO_3 and 32 percent HNO_3.

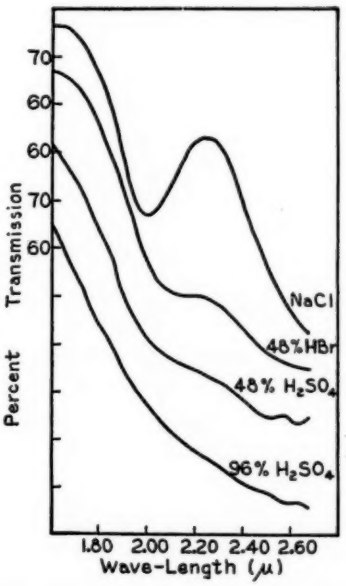

FIG. 2. Percent transmission of NaCl solution saturated at 23°C, 48 percent HBr, 48 percent H_2SO_4 and 96 percent H_2SO_4.

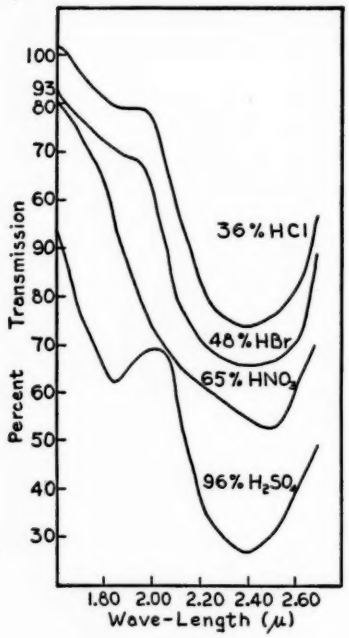

FIG. 3. Transmission in region of 2.40μ of 36 percent HCl, 48 percent HBr, 65 percent HNO_3, and 96 percent H_2SO_4, as compared to that of H_2O.

in the gaseous form. The band at about 3.8μ for HBr also failed to appear.

Fig. 4 shows the transmission of H_2O and solutions of 45 percent HF, 36 percent HCl, and 48 percent HBr in the region of 5.0μ to 6.5μ. In addition to the bands which are observed in water, there is a strong band at about 5.5μ, which was found for all the acid solutions. The intensity of this band is greater even than that of the strong 6.18μ water band, as can be seen in Fig. 4 by an examination of the absorption maxima for the solutions at 5.5μ as compared with the absorption of water at 6.18μ. The centers of the bands for the solutions correspond only approximately and there is a gradual shift to the longer wave-lengths as the halogen ion increases in atomic weight, the bands for HCl and HBr being much sharper than that of HF. The difference in shape of the HF band may be due to the presence of both HF and H_2F_2 in the solution. Fig. 5 shows a comparison of the transmission of water with that of solutions of 0.5 percent C_6H_5COOH, 90 percent HCOOH, 65 percent HNO_3, and 96 percent H_2SO_4. These solutions show absorption in the same region as

TABLE I.

Solutions	Observed bands	Solutions	Observed bands
HBr	5.52μ	HCOOH	5.62μ
HCl	5.48	H_2SO_4	5.58
HF	5.46	HNO_3	5.62
C_6H_5COOH	5.60		

the other acids shown in Fig. 4, but the bands have been shifted to longer wave-lengths and the maxima occur at about 5.6μ. Table I gives the position of the observed bands. There is a marked difference in intensity for this band in these acids. This difference in intensity is, no doubt, in part due to the difference in concentration of the various solutions, and the very low intensity of the band observed for the benzoic acid solution can be accounted for in this way. The relation between the transmission of H_2O, and saturated solutions of NaBr and NaCl was studied. These salts do not show the strong band at 5.5μ which has been observed in the case of the acids. In fact, the curves show only the water bands, and correspond as well as

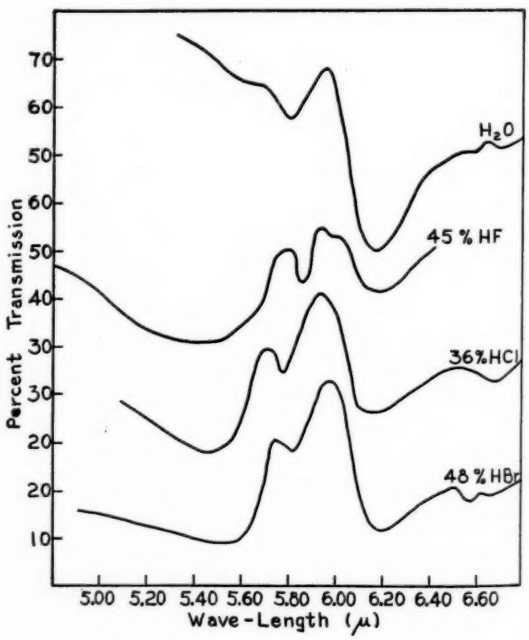

FIG. 4. Percent transmission of H_2O, 45 percent HF, 36 percent HCl and 48 percent HBr.

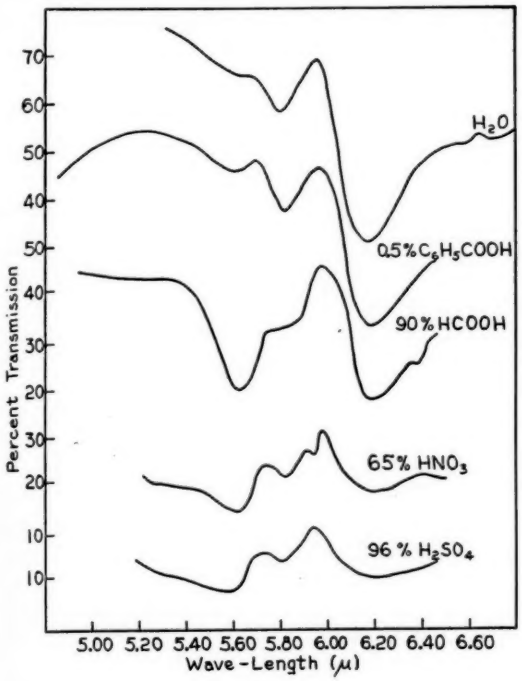

FIG. 5. Percent transmission of H_2O, 0.5 percent C_6H_5COOH, 90 percent HCOOH, 65 percent HNO_3 and 96 percent H_2SO_4.

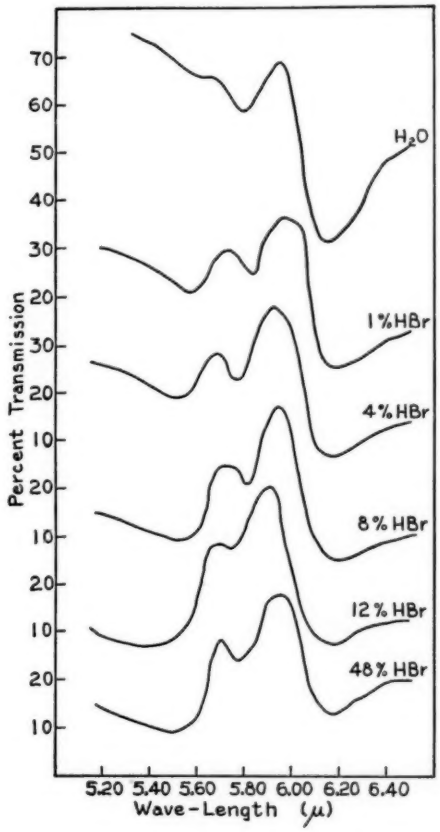

FIG. 6. Percent transmission of H_2O and 1 percent, 4 percent, 8 percent, 12 percent and 48 percent HBr.

separate observations made upon water check with each other.

As was noted above, HCl and HBr in solution do not give the strong absorption bands at 3.5μ and 3.8μ, respectively, which are found for these substances in the gaseous form. On account of the general similarity of the absorption bands in the region of 5.5μ due to the acid solutions, it is probable that they have a like origin. Since the only common constituent of the acids is the hydrogen atom, the bands must be caused by either the whole molecule attached to a water molecule through the hydrogen atom, or the hydrogen ion attached to a water molecule. If the latter case is true, then the observed differences in position and shape of these bands must be attributed to the influence of the negative ion at close distances to the $H_3{}^+O$. In order to test this point, a series of observations was taken on the transmission of HBr at concentrations from 1 to 48 percent. These results are shown in Fig. 6. As can be seen, there is no appreciable change in the position of this band with concentration. From this check and other experimental work,[4] it seems probable that the vibrational energy levels observed in the region of 5.5μ are due to the vibration of the acid molecule as a whole against the water molecule when attached to a water molecule through the hydrogen of the acid. This interpretation may seem inconsistent with not finding the bands at 3.5μ and 3.8μ for HCl and HBr, respectively. However, this inconsistency may be explained by considering the changes in the vibrational energy which take place in the hydrated acid molecule. This may well cause a shift of the band to longer wave-

[4] In hydrolizing salts, such as $ZnCl_2$ and Na_2CO_3, it has been recently found that the 5.5μ acid band is intense when the solution gives a hydroxide test and is of very low intensity when the solution gives an acid test. This indicates that this band is due to the presence of the undissociated acid molecule.

lengths. In work with the Raman effect, shifts have been found[5] in the spectral lines which correspond to the absorption bands at 9.5μ and 11μ for solutions of HNO_3 and H_2SO_4, respectively. These bands may be due to the new vibration of the acid molecule in solution rather than to the vibrational frequency of the molecule in the gaseous state. Further work is now in progress in order to see if all acids have their absorption bands as observed in the gaseous state shifted to longer wave-lengths when in solution.

In Fig. 6 it is of interest to note that the 5.5μ band is still present even with a one percent solution of HBr. The intensity of the band seems to vary directly as the concentration, without any sudden change, but to decide this point more definitely a very detailed study must be made.

[5] S. K. Mukherjee and P. N. Sengupta, Ind. J. Phys. **3**, 503 (1929); I. R. Rao, Nature **124**, 762 (1929).

The Raman Spectra and Molecular Constants of the Hexafluorides of Sulfur, Selenium and Tellurium

DON M. YOST, CARSTEN C. STEFFENS AND SIEGFRIED T. GROSS, *Gates Chemical Laboratory, California Institute of Technology**

(Received February 19, 1934)

The Raman spectra of the gaseous and liquid hexafluorides of sulfur, selenium and tellurium were determined (Table I). Three lines for each substance were observed and this is the number permitted by the selection rules for a regular octahedral molecule. Frequency formulae based on central forces were derived, and these, together with the appearance of the spectra, were used to assign the observed frequencies to the proper modes of vibration. Estimates of the magnitudes of the forbidden frequencies were made. A provisional value of $-238{,}000$ cal. is given for the free energy of formation of SF_6 (g) at 25°.

INTRODUCTION

THE hexafluorides of the sulfur group elements have been shown by electron diffraction experiments to consist of highly symmetrical molecules, the six fluorine atoms occupying the corners of a regular octahedron with the remaining atom at the center.[1] No spectroscopic measurements to determine the fundamental molecular frequencies have been made, and further information regarding bond strengths and thermodynamic quantities requires such data. As one step in obtaining such material, the Raman spectra of these substances in both liquid and gaseous forms were determined.

Redlich, Kurz and Rosenfeld[2] have derived, as a function of central force constants, formulae for the fundamental modes of vibration of the regular octahedral molecule, but they oversimplified the problem in ignoring the forces present in the equilibrium positions of the atoms. It was therefore necessary to treat the problem more thoroughly. The results of both the theoretical and experimental studies are presented in this paper.

We wish to express here our appreciation to Professor Roscoe G. Dickinson for valuable suggestions made in connection with the technique for determining the Raman spectra of gases, and to Dr. E. B. Wilson, Jr., who applied Placzek's[3] theory of scattering to deduce the selection and polarization rules for the octahedral type molecule.

THEORETICAL

The methods of general dynamics which were developed for the treatment of systems involving more coordinates than degrees of freedom are commonly applied only in case the differential equations of constraint are non-integrable. The same methods are applicable regardless of the integrability of the equations of constraint; but in the integrable cases, as many coordinates as there are equations of constraint can be eliminated, thereby reducing the number of differential equations. If the physical system is highly symmetrical, the corresponding high symmetry of the differential equations may compensate the greater number of equations in the set, as was pointed out by Routh.[4] Since the system considered in this paper is highly symmetrical, the procedure usually applied to non-holonomic systems will be used.

The Lagrangian equations of motion for a non-holonomic system are:

* Contribution No. 400.

[1] Pauling and Brockway, Proc. Nat. Acad. **19**, 68 (1933).

[2] Redlich, Kurz and Rosenfeld, Zeits. f. physik. Chemie **B19**, 231 (1932).

[3] Cf. Debye, *The Structure of Molecules*, p. 86, Blackie and Son, London, 1932.

[4] E. J. Routh, *Advanced Rigid Dynamics*, p. 31, Macmillan and Co., N. Y., 4th Ed., 1884.

$$\frac{d}{dt}\frac{\partial L}{\partial \dot{q}_i}-\frac{\partial L}{\partial q_i}=\sum_{j=1}^{m}\lambda_j\frac{\partial {}_jf}{\partial q_i},$$

where ${}_jf=0$ for $j=1, 2, \cdots m$ are the m equations of constraint, and the λ_j's are m undetermined multipliers. The n equations of motion plus the m equations of constraint determine the n coordinates and m λ_j's.

An isolated system of point particles, where L equals $T-V$ and is not a function of the time, has six integrals of linear and angular momentum, providing six equations of constraint. These momenta will be assumed zero. The motion of the system will be described with s sets of rectangular coordinates, derivable from one another by translation, whose origins are at the positions of the particles when the system is in an equilibrium configuration.

The potential energy V may be expanded in a Maclaurin's series in n variables about the equilibrium configuration. Third and higher powers are neglected. The condition that $\partial V/\partial q_i=0$ in an equilibrium configuration does not follow in general from the equations of motion, since these partial derivatives are related, not to the total force along the corresponding coordinates, but only to that part of the force due to reactions included in L as distinguished from reactions included in the equations of constraint. If, however, an equilibrium configuration of the system is unaffected by the absence of the constraints, or, from another viewpoint, if the constraints exert no forces in the equilibrium configuration, then *in that configuration* $\partial V/\partial q_i=0$. These partial derivatives are therefore the negatives, not only of the components of that part of the forces included in L, but also of the total forces along the corresponding coordinates. In the systems of interest, the potential energy is $2V=\sum_{i=1}^{n}\sum_{j=1}^{n}b_{ij}q_iq_j$.

Since the kinetic energy T of the system is the sum of the kinetic energies of the particles composing it, and since the coordinates for each particle are orthogonal, no cross-products will appear. The kinetic energy is $2T=\sum_{i=1}^{n}a_i\dot{q}_i^2$ where the a_i's are constants.

The equations of constraint are homogeneous linear functions of the coordinates, ${}_jf=\sum_{i=1}^{n}{}_jf_iq_i=0$. The undetermined multipliers may be written as ${}_0\lambda_j+{}_1\lambda_j$ where ${}_0\lambda_j$ is the value of λ_j in the equilibrium configuration.

The equations of motion are solved by the usual substitution $q_i=A_ie^{\mu t}$ and ${}_1\lambda_i=-M_ie^{\mu t}$. The resulting relations are:

$$(a_i\mu^2+b_{ii})A_i+\sum_{\substack{j=1\\ j\neq i}}^{n}b_{ij}A_j+\sum_{r=1}^{6}{}_rf_iM_i=0 \qquad i=1, 2, \cdots n,$$

$$\sum_{i=1}^{n}{}_rf_iA_i=0 \qquad r=1, 2, \cdots 6.$$

The ${}_0\lambda_r$'s are all zero since the equations of motion must be satisfied when the variables and their derivatives are all zero.

The secular determinant is bordered by six rows and six columns of constants. It is of the $(n+6)$th order and of the $(n-6)$th degree in the variable, μ^2, which is confined to the non-zero terms of the principal diagonal. Since a row or column from the border may be used as an operator without disturbing any of the bordering elements, and since these elements are simple, the determinant is comparatively easy to factor. The secular determinant of a system of seven particles arranged in a regular octahedron is a "block circulant," and is immediately factorable into three determinants, each of order $(n+6)/3$.[5]

The seven particles, 0, 1, $\cdots 6$, are placed in a rectangular coordinate system at 000, $a00$, $0a0$, $\bar{a}00$, $0\bar{a}0$, $00a$, and $00\bar{a}$, respectively. k_{01}, k_{12}, and k_{24} denote force constants due to reactions between the central and a peripheral particle, between two adjacent peripheral particles, and between two opposite peripheral particles, respectively. m_0 and m_1 denote the mass of the central and of any peripheral particle, respectively. $-b$, $-h$, and $-j$ denote ratios of forces to corresponding equilibrium distances, where the forces are those at equilibrium due to reaction between the central and a peripheral particle, between two adjacent peripheral particles, and between two opposite peripheral particles, respectively. There is a relation, $b=-4h-2j$, between these constants.

The kinetic and potential energies of the system for infinitesimal displacements and velocities are given by the following equations.

[5] Muir and Metzler, *Theory of Determinants*, p. 485, privately printed, Albany, N. Y., 1930.

$$2T=m_0(\dot{x}_0^2+\dot{y}_0^2+\dot{z}_0^2)+m_1(\dot{x}_1^2+\dot{y}_1^2+\dot{z}_1^2+\dot{x}_2^2+\dot{y}_2^2+\cdots+\dot{z}_6^2),$$

$$\begin{aligned}2V=&k_{01}[(x_1-x_0)^2+(x_3-x_0)^2+(y_2-y_0)^2+(y_4-y_0)^2+(z_5-z_0)^2+(z_6-z_0)^2]+b[(x_2-x_0)^2+(x_4-x_0)^2\\&+(x_5-x_0)^2+(x_6-x_0)^2+(y_1-y_0)^2+(y_3-y_0)^2+(y_5-y_0)^2+(y_6-y_0)^2+(z_1-z_0)^2+(z_2-z_0)^2\\&+(z_3-z_0)^2+(z_4-z_0)^2]+(k_{12}/2)[(x_1-y_1-x_2+y_2)^2+(x_1-z_1-x_5+z_5)^2+(x_1+y_1-x_4-y_4)^2\\&+(x_1+z_1-x_6-z_6)^2+(y_2-z_2-y_5+z_5)^2+(x_2+y_2-x_3-y_3)^2+(y_2+z_2-y_6-z_6)^2+(x_3-z_3-x_6+z_6)^2\\&+(x_3-y_3-x_4+y_4)^2+(x_3+z_3-x_5-z_5)^2+(y_4+z_4-y_5-z_5)^2+(y_4-z_4-y_6+z_6)^2]\\&+(h/2)[(x_1+y_1-x_2-y_2)^2+(x_1-z_1-x_6+z_6)^2+(x_1-y_1-x_4+y_4)^2+(x_1+z_1-x_5-z_5)^2\\&+(y_2+z_2-y_5-z_5)^2+(x_2-y_2-x_3+y_3)^2+(y_2-z_2-y_6+z_6)^2+(x_3+z_3-x_6-z_6)^2+(x_3+y_3-x_4-y_4)^2\\&+(x_3-z_3-x_5+z_5)^2+(y_4-z_4-y_5+z_5)^2+(y_4+z_4-y_6-z_6)^2]+h[(x_2-x_5)^2+(x_5-x_4)^2+(x_4-x_6)^2\\&+(x_6-x_2)^2+(y_1-y_6)^2+(y_6-y_3)^2+(y_3-y_5)^2+(y_5-y_1)^2+(z_1-z_2)^2+(z_2-z_3)^2+(z_3-z_4)^2\\&+(z_4-z_1)^2]+k_{24}[(x_1-x_3)^2+(y_2-y_4)^2+(z_5-z_6)^2]+j[(x_2-x_4)^2+(x_5-x_6)^2+(y_1-y_3)^2+(y_5-y_6)^2\\&+(z_1-z_3)^2+(z_2-z_4)^2].\end{aligned}$$

The six integrals of linear and angular momenta equated to zero give the six following equations.

$$\begin{aligned}m_0x_0+m_1(x_1+x_2+x_3+x_4+x_5+x_6)&=0, & y_5-y_6-z_2+z_4&=0,\\m_0y_0+m_1(y_1+y_2+y_3+y_4+y_5+y_6)&=0, & x_5-x_6-z_1+z_3&=0,\\m_0z_0+m_1(z_1+z_2+z_3+z_4+z_5+z_6)&=0, & x_2-x_4-y_1+y_3&=0.\end{aligned}$$

The secular determinant is set up from these equations and solved. The roots determine the following six frequencies, the multiplicity being given by the figure in parenthesis.

$$4\pi^2\nu_1^2(1)=(k_{01}+4k_{12}+2k_{24})/m_1, \quad (1) \qquad 4\pi^2\nu_3^2(3)=(2k_{12}-2h)/m_1, \quad (3)$$

$$4\pi^2\nu_2^2(2)=(k_{01}+k_{12}+2k_{24}+3h)/m_1, \quad (2) \qquad 4\pi^2\nu_4^2(3)=(k_{12}+h-2j)/m_1, \quad (4)$$

$$4\pi^2\nu_{5,6}^2(3)=\frac{1}{2m_0m_1}\{A\pm[A^2+4m_0(m_0+6m_1)(-k_{01}k_{12}+3k_{01}h+2k_{01}j+4(2h+j)(k_{12}+h))]^{\frac{1}{2}}\},$$

$$A=(m_0+2m_1)k_{01}+3m_0k_{12}-(m_0+16m_1)h-2(m_0+4m_1)j, \quad (5)$$

$$\nu_1^2=\nu_2^2+(3/2)\nu_3^2. \quad (6)$$

Another set of frequency formulae for the octahedral XY_6 molecule was derived by Dr. E. B. Wilson, Jr., using a very restricted type of valence-force potential function involving only three constants, k_{01} the $X-Y$ force constant, p the interaction constant for the effect of extension of the $X-Y$ bond, and k_φ the constant for the bending of the valence bonds. A more thorough treatment would, of course, introduce further constants. The formulae are the following:

$$4\pi^2\nu_1^2(1)=(k_{01}+4p)/m_1, \quad (7) \qquad 4\pi^2\nu_3^2(3)=4k_\varphi/m_1, \quad (9)$$

$$4\pi^2\nu_2^2(2)=(k_{01}-2p)/m_1, \quad (8) \qquad 4\pi^2\nu_4^2(3)=2k_\varphi/m_1, \quad (10)$$

$$4\pi^2\nu_{5,6}^2(3)=\frac{1}{6m_1(1+4m_1/m_0)}\left\{B\pm\left[B^2-48\left(1+\frac{4m_1}{m_0}\right)\left(1+\frac{6m_1}{m_0}\right)^2k_{01}k_\varphi\right]^{\frac{1}{2}}\right\}, \quad (10)$$

$$B=24\frac{m_1^2}{m_0^2}k_{01}+6\left(1+\frac{4m_1}{m_0}\right)^2k_\varphi+2\left(1+\frac{4m_1}{m_0}\right)(k_{01}+k_\varphi), \quad (11)$$

$$\nu_3/\nu_4=2^{\frac{1}{2}}. \quad (12)$$

Of these six frequencies, ν_1, ν_2, and ν_3 are permitted by the Raman selection rules, and the two latter will be depolarized equally with $\rho = 6/7$. The modes of vibration are pictured in Fig. 1 and are in agreement with those described by Redlich, Kurz and Rosenfeld.[2]

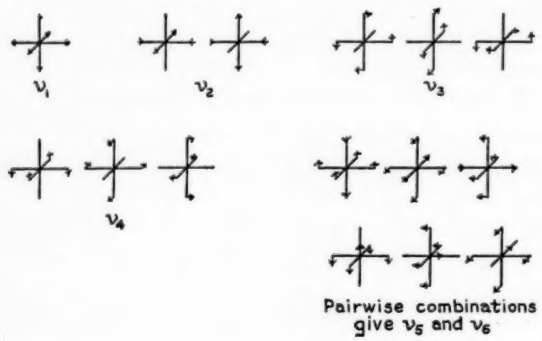

FIG. 1. Fundamental modes of vibration of regular octahedral model of XY_6.

EXPERIMENTAL

The hexafluorides were prepared by treating elementary sulfur, selenium, and tellurium with gaseous fluorine. The methods of purification have been described elsewhere.[6] About two days were required for the preparation of each compound.

In the experiments on the liquids, the material was contained in a Pyrex glass tube 1 cm in diameter equipped at one end with a plane glass window and at the other with a right cone of black nickel-oxide Pyrex glass. The tube was supported vertically in a Dewar flask silvered on one-half of its circumference. Cooled alcohol or ice-water served as low temperature baths. In all cases the liquids were under pressures varying from five to nine atmospheres. The selenium and tellurium compounds were run at 0°, and that of sulfur at −50°. A mercury arc in Pyrex served as a source of radiation.

The strongest Raman line appeared after an exposure of twenty minutes, but to obtain all of the lines two or three hours were necessary. In no case were more than three lines observed resulting from a single exciting frequency. For a given exposure time, the Raman lines from tellurium hexafluoride were the most intense and those from the sulfur compound the least.

In the experiments on the gaseous hexafluorides, quartz was used throughout. The spectrograph contained in it a dish of mercury whose vapor served to absorb a large fraction of the 2537A radiation used to excite the spectra. The tube containing the gases was 2.5 cm in diameter, and 30 cm long. It was equipped with a 1.3 cm diameter window at one end, and a right cone, covered with optical black paint to prevent reflections, at the other. The gases were present at a pressure of about 75 lbs./sq. in.

The lengths of the exposures for the gases varied from a half hour to thirty hours. Tellurium hexafluoride yielded three Raman lines. The one of greatest $\Delta\nu$ was strong and sharp with only a trace of diffuseness on the long wave-length side. The weakest line had a well-defined center and faint, diffuse wings. The line of least $\Delta\nu$ was broad (19 cm^{-1}) and uniformly intense over most of its width, and appeared also as anti-Stokes radiation. The other two gases yielded only one strong sharp line each. For a given length of exposure, the most intense lines were obtained from tellurium hexafluoride and the least intense from the sulfur compound.

The lines obtained from the liquids were appreciably broader than those from the gases. The accuracy attained for the former was about ± 3 cm^{-1} and for the strongest line of the latter ± 0.1 cm^{-1}.

RESULTS OF EXPERIMENTS

The results of the experiments are presented in Table I, together with the interatomic distances obtained from electron diffraction experiments.[1] The numbers in parenthesis adjoining the symbols ν are multiplicities, those adjoining the frequency values are relative intensities.

Only three lines are permitted by the selection rules and this is the number observed.

As the table shows the frequency ν_1 has nearly the same value for the gases as for the liquids, a result that is usually found for nonpolar substances.[7] The highly symmetrical hexafluoride molecules evidently do not interact with each

[6] Yost and Claussen, J. Am. Chem. Soc. **55**, 885 (1933).

[7] Kohlrausch, *Der Smekal Raman Effekt*, p. 126, Julius Springer, Berlin, 1931.

TABLE I. *The Raman frequencies of sulfur, selenium and tellurium hexafluorides.*

Substance	State	$\nu_1(1)$ cm^{-1}	$\nu_2(2)$ cm^{-1}	$\nu_3(3)$ cm^{-1}	$M-F$ A	$I\times10^{40}$
SF_6	Liquid	776(10)	642(2)	522(2)		
	Gas	772.4			1.58	311.5
SeF_6	Liquid	710(10)	662(2)	405(2)		
	Gas	708.0			1.70	362.5
TeF_6	Liquid	697(10)	672(2)	316(4)		
	Gas	701.2(10)	674.4(1)	313*(4)	1.84	425.0

$M-F$ = distance from S, Se, or Te to F.
I = moment of inertia in g·cm^2.
* The width is about 19 cm^{-1}.

other in such a way as to affect appreciably the valence forces, although the bonds themselves may be ionic in character.

The assignment of the strongest line from each substance to the completely symmetrical mode of vibration, $\nu_1(1)$ is in accord with the theory[3] and is almost certainly correct. In the case of the gases, the strongest line is also sharp with only a trace of diffuseness on the long wave-length side. This indicates a Q branch and is to be expected from the mode of vibration, $\nu_1(1)$. The weakest line from tellurium hexafluoride was assigned to ν_2, and has a well-defined center with less intense, diffuse wings on either side which were, however, rendered somewhat indistinct by the continuous background. The broad line is moderately intense and is assigned to ν_3. The broadness is doubtless due to unresolved rotational structure, and the uniform intensity over its width indicates the presence of P, Q and R branches. These considerations, together with the relative magnitudes of the frequencies to be expected from the modes of vibration involved, would seem to confirm the assignments given to the lines. To render them more certain the constant-free relation, Eq. (6), between the allowed frequencies was employed.

From the relation, $\nu_1^2=\nu_2^2+(3/2)\nu_3^2$, it is evident that ν_1 is the greatest of the three frequencies. It was found that the best agreement was obtained when the smallest frequency was assigned to ν_3. The values of $(\nu_2^2+(3/2)\nu_3^2)^{\frac{1}{2}}$ are from 10 percent to 17 percent greater than those observed for ν_1, the best agreement being obtained with tellurium hexafluoride. The assignments are, therefore, in agreement with the best available criteria. It must be pointed out that polarization experiments would be of little assistance in this case since the depolarization factor, ρ, will be the same for ν_2 and ν_3.

THE FORCE CONSTANTS AND FORBIDDEN FREQUENCIES

Both sets of frequency formulae were used to estimate the magnitudes of the forbidden frequencies. The values so calculated are to be regarded as rough approximations only. They would serve as a guide in the analysis of absorption spectra.

The data are insufficient to determine all the constants of Eqs. (1–5). From the relation discovered by Professor R. M. Badger[8] of this laboratory it is possible to determine, at least approximately, the values of k_{01}, and, with less certainty, k_{12}. k_{24} is certainly small and is disregarded. h may be calculated from ν_2 alone, and elementary inverse square law considerations show that $j=h/(2)^{\frac{1}{2}}$. k_{01} and k_{12} were used to calculate ν_1 in order to test the approximate correctness of the constants. The agreement with experiment is not exact but is satisfactory. The results of the calculations are represented in Table II. The negative values for h and j indicate the existence of repulsive forces between fluorine atoms.

TABLE II. *Estimated force constants and forbidden frequencies. Eqs. (1–5) (central forces).*

Substance	k_{01} $\times10^{-5}$	k_{12} $\times10^{-5}$	ν_1 calc.	ν_1 obs.	$-h$ $\times10^{-5}$	Estimated forbidden frequencies ν_4	ν_5	ν_6
SF_6	5.9	0.50	844	772	1.0	280	620	1510
SeF_6	5.8	0.36	807	708	0.55	230	570	960
TeF_6	5.9	0.26	790	701	0.28	190	420	850

The ν's are expressed in cm^{-1} and the constants in dynes/cm.

Similar calculations were made using Eqs. (7–11). The three constants were determined in this case directly from the experimental data. The results are presented in Table III.

It does not appear possible to make a definite choice between the kinds of bonds postulated in

[8] Private communication.

TABLE III. *Estimated forbidden frequencies Eqs. (7–11) (valence bonds).*

Substance	k_{01} $\times 10^{-5}$	p $\times 10^{-5}$	k_{φ} $\times 10^{-5}$	ν_4 cm^{-1}	ν_5 cm^{-1}	ν_6 cm^{-1}
SF_6	5.30	0.344	0.765	370	540	970
SeF_6	5.15	0.123	0.460	286	430	650
TeF_6	5.23	0.086	0.274	222	310	610

deriving the two sets of frequency formulae. That the bonds are not of the extreme ionic type seems likely in virtue of the fact that the spectra are readily obtained.

Of the three frequencies forbidden in the Raman effect, ν_5 and ν_6 should be observed in infrared absorption experiments. Specific heat measurements on the gaseous hexafluorides would also add considerably to our knowledge concerning the magnitudes of the unknown frequencies.

THERMODYNAMIC CONSTANTS

The virtual entropy of sulfur hexafluoride may be expressed as $S^*_{298^\circ}=S_a+S_f$, where S_f is the entropy associated with the forbidden frequencies and S_a the remaining entropy. The value of S_a is 64.6 cal./deg., and it was calculated from the data in Table I. The symmetry number is 24. S_f was estimated by using the first set of calculated values for the forbidden frequencies, and has the provisional value 5.9 cal./deg. $S^*_{298^\circ}$ becomes then 70.5 cal./deg. The entropy of fluorine is 48.0 cal./deg.,[9] and that of rhombic sulfur is 7.6 cal./deg.[10] at 25° and 1 atmosphere. The heat of formation of sulfur hexafluoride at constant pressure and 25° is 262,000 cal.[6] When these values are combined, the following equation can be written.

$$S\ (\text{rhombic})+3F_2(g)=SF_6(g)$$
$$\Delta H=-262{,}000\ \text{cal.}\quad \Delta S_{298}=-81\ \text{cal./deg.}$$
$$\Delta F^\circ_{298}=-238{,}000\ \text{cal.}$$

It is believed that the error in this provisional value of ΔF°_{298} is due principally to that in ΔH, namely, ± 3000 cal. As an application of this free energy value, it may easily be shown that sulfur hexafluoride has a large tendency to hydrolyze when brought into contact with water, but due to the extreme slowness of the reaction, no hydrolysis is observed. However, it may be predicted that no hexafluoride will result when sulfuric and hydrofluoric acids are mixed, and this is in agreement with experiment.

[9] Yost and Hatcher, J. Chem. Educ. **10**, 330 (1933).

[10] Lewis and Randall, *Thermodynamics*, p. 464, McGraw-Hill Book Co., N. Y., 1923.

Modified Scattering by Crystalline HCl and HBr

DIXON CALLIHAN AND E. O. SALANT, *Department of Physics, Washington Square College, New York University*

(Received April 9, 1934)

The values of the modified frequencies of radiation scattered by crystalline HCl and HBr at temperatures just below their freezing points are found to be 2784 cm^{-1} and 2480 cm^{-1}, respectively, for the long wave edge. As with gases and liquids, the intensities of scattering are in the reverse order of intensities of absorption and the difference in the Raman shifts with change of state is too great to be attributed to Lorentz-Lorenz forces alone. The Raman band of crystalline HCl corresponds to the high frequency branch of two absorption bands found by Hettner, not to the center of the bands; on the possibility that, because of this correspondence, this branch is a *Q*-branch, the temperature variations of the absorption bands and the heat capacity at low temperatures can be accounted for. The non-existence of a third branch, for the *R*, is noted.

MODIFIED scattering by gaseous HCl has been reported by Wood[1] and Wood and Dieke,[2] by gaseous HBr and HI and liquid HCl and HBr by Salant and Sandow.[3] This paper is concerned with the modified scattering by crystalline HCl and HBr; the Raman shifts of the centers of these bands have already been recorded.[4]

Apparatus and Experimental Results

A Hilger constant deviation spectrograph with the small camera (17 cm focus lens) having a dispersion of 356 cm^{-1}/mm at λ4550 was used, which, with the violet group of lines of a commercial six inch mercury arc (3 amp., 130 volts across the arc terminals) focussed into the crystals, gave Raman lines in half an hour and less with Eastman I–J plates.

The arrangement was the usual one according to Wood,—the cell, 6 cm×1.5 cm diameter, being placed horizontally in a Dewar flask with a concave mirror on the side of the cell opposite the arc.

The scattered lines fall somewhat long of λ4358, in a region of considerable continuous background from the incident spectrum, which tends to obscure weak Raman lines. This continuous radiation and also the λ4358 group were reduced greatly by a filter of 0.25 g of methyl violet in a liter of water, without reducing the intensities of λλ4047 and 4078 appreciably.

HCl was prepared from NaCl and H_2SO_4, then dried in H_2SO_4 and condensed in the cell. HBr was generated by heating NaBr in syrupy H_3PO_4, then passed over red phosphorus, dried by $CaCl_2$ and P_2O_5 and passed through cooled traps into the cell. Perfectly clear crystals were obtained and kept several hours. The temperatures in the crystals were a few degrees below the freezing points. In attempted experiments with HI, dissociation occurred too rapidly to obtain lines.

Spectrograms and microphotometer curves of the Raman lines are reproduced in Figs. 1 and 2 respectively. In the latter is included a curve of a liquid HCl line obtained during these experiments, appearing much sharper than that previously reported,[3] though the two were microphotometered under identical conditions. The broadness of the earlier curve is attributed to continuous background, which is removed by the filter in the present experiments.

The lines, as may be seen from the curves, appear broad; the average values of the shifts of the edges from the parent lines being:

	Long wave edge vac. cm^{-1}	*Short wave edge* vac. cm^{-1}
HCl	2784±3	2743±4
HBr	2480±3	2449±4

These values were determined by a Hartmann interpolation formula using 24,705 and 24,516

[1] R. W. Wood, Phil. Mag. **7**, 744 (1929).
[2] R. W. Wood and G. H. Dieke, Phys. Rev. **36**, 1355 (1930).
[3] E. O. Salant and A. Sandow, Phys. Rev. **37**, 373 (1931).
[4] E. O. Salant and D. Callihan, Phys. Rev. **43**, 590 (1933).

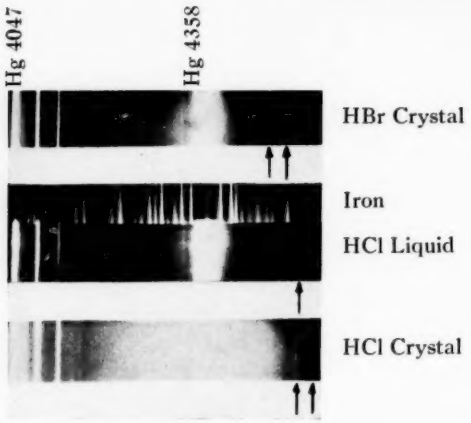

FIG. 1. Spectrograms of Raman lines.

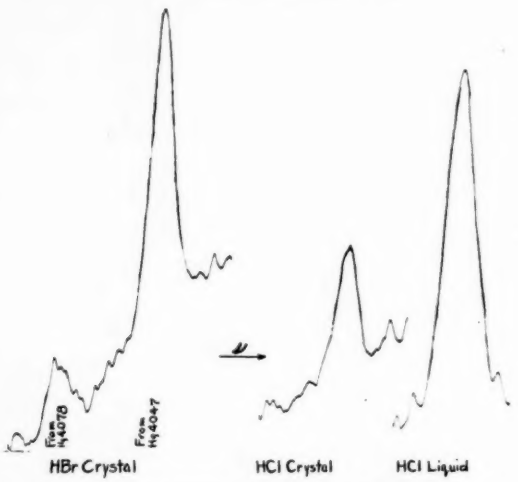

FIG. 2. Microphotometric tracings of Raman lines.

cm^{-1} for λλ4047 and 4078. As with the gas and liquid states, the order of intensities is HCl<HBr.

The separation of the two Raman lines (equal to the difference between λλ4047 and 4078) on each spectrogram, is conclusive identification of the parent lines, so that the shift corresponds in order of magnitude to the (1←0) vibration of the molecules as given by Raman and infrared data[5] in the gaseous states.

The difference between the Raman frequencies of gaseous and solid HCl is too great to be entirely due to Lorentz-Lorenz forces, as calculated according to Breit and Salant.[6] The calculation gives approximately 3 cm^{-1} for HCl as compared to the experimental value 102 cm^{-1}. The calculated value of the Lorentz-Lorenz displacement for HBr would be about the same as that of HCl and hence is much smaller than the 78 cm^{-1} measured result. A similar conclusion was drawn from comparison of gaseous and liquid data.[3]

The positive results obtained from these scattering experiments lend weight to the nature of the crystalline structure of the hydrogen halides as non-ionic, contrary to that given by Natta.[7]

DISCUSSION

It may be superfluous to remind the reader that the "Stokes" Raman band of a diatomic molecule is a Q branch and consequently the value of its high frequency edge (that is, the frequency difference between the exciting line and the long wave edge of the band as it appears on the plate) is the value of the (1←0) rotationless vibrational transition and that, consequently, this edge coincides with the center of the vibration-rotation band as it appears in absorption. This is seen clearly in the Raman bands of the gases of HCl and HBr.[1, 2, 3]

In Fig. 3 (a) are reproductions of absorption bands of crystalline HCl measured by Hettner[8] and of a microphotometric tracing of the Raman band of crystalline HCl measured by us. (There is no relation between their respective ordinates.) Surprisingly, the high frequency limit of the Raman band, 2784 cm^{-1}, agrees, not with the center of the two absorption bands, as would be expected if the two bands are P and R branches, but with the high frequency edge of the 2753 cm^{-1} band. It might be concluded that the 2753 cm^{-1} band is, accordingly, a Q and not an R branch; or, if the motions of the molecule transverse to its axis are vibratory rather than rotatory, that the 2784 cm^{-1} band represents the frequency ν_1 of motion along the axis and not the combination $\nu_1+\nu_2$, where ν_2 is the frequency of motion transverse to the axis. (The band at 2712 cm^{-1} would be the P branch, or $\nu_1-\nu_2$, on either interpretation of 2753.) But then the R branch, or $\nu_1+\nu_2$, should appear at about 2856 cm^{-1}, and no such band is recorded by Hettner.

[5] C. F. Meyer and A. A. Levin, Phys. Rev. **34**, 44 (1929); W. F. Colby, Phys. Rev. **34**, 53 (1929).

[6] G. Breit and E. O. Salant, Phys. Rev. **36**, 871 (1930).

[7] G. Natta, Nature **127**, 235 (1931).

[8] G. Hettner, Zeits. f. Physik **78**, 141 (1932).

Nevertheless, this interpretation does remove a number of difficulties. Hettner pointed out that at $T=87°K$ the 2753 cm^{-1} band is less intense than the one at 2712 cm^{-1}, an impossible intensity relation if the bands are P and R branches; if the selection rules are modified (by the intermolecular fields) so as to permit Q transitions, the P branch may be expected to be the more intense. Furthermore, the relative weakness of the 2712 cm^{-1} band at $T=20°K$, noted by Hettner, is to be expected if it is a P and the other a Q branch. Hettner noted that the frequency ν_2, obtained from regarding the 2753 cm^{-1} band as $\nu_1+\nu_2$, led to impossibly large heat capacities at low temperatures. But if $\nu_1=2784$ cm^{-1}, then $\nu_2=72$ cm^{-1}, and the contributions of this motion to the molecular heat capacity at constant volume always lie below the values calculated by Clusius[9] from his experimental data for C_p, as they should. This appears in Fig. 4, where both $\frac{2}{3}$ Einstein and $\frac{2}{3}$ Debye heat capacity functions of $\theta=103°$ ($\nu=72$ cm^{-1}) are plotted ($\frac{2}{3}$ for two degrees of freedom). The close correspondence of the Debye curve with the measured heat capacities over a considerable range of lower temperatures is to be observed.[10]

In Fig. 3 (a) and (b) are shown reproductions of Hettner's curves at $T=87°K$ and $T=20°K$ drawn to the same scale. It is seen that, as the temperature is lowered, the maximum of the high frequency band shifts to *higher* frequencies, which it should if it is a Q branch, whereas it would shift to lower frequencies were it an R branch.

Thus, calling the quantum number governing the transverse motions of the molecule, j, and understanding that j may refer either to complete rotations or to pendulum motions of large or small amplitude, it would seem that, for this vibrational transition of HCl molecules in the crystalline state, $\Delta j \lesseqgtr 0$, but that transitions $\Delta j>0$ are forbidden. It is certainly not obvious how this is possible, but alternative suggestions

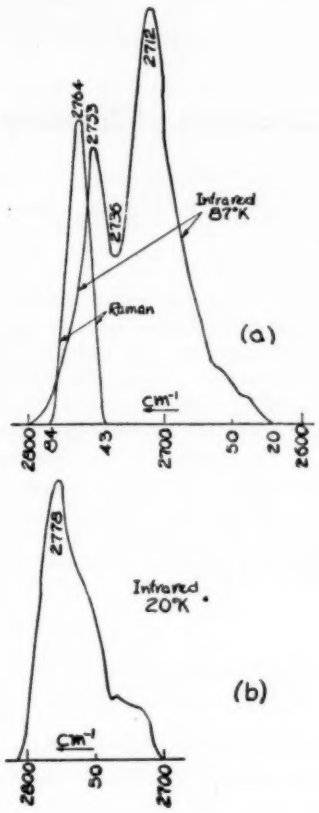

FIG. 3.

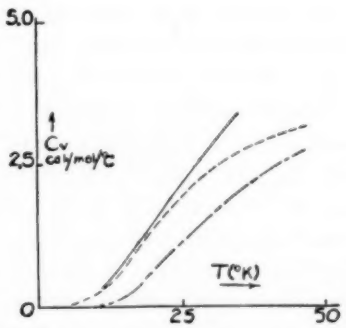

FIG. 4. Unbroken curve, experimental C_v; curve with even dashes, $C_v=\frac{2}{3}$ Debye function $\nu=72$ cm^{-1}; curve with long and short dashes $C_v=\frac{2}{3}$ Einstein function $\nu=72$ cm^{-1}.

considered to explain coincidence of the 2753 cm^{-1} absorption band and the Raman band gave impossible values of the heat capacity at low temperatures and the wrong behavior of the absorption bands with change of temperature.

We are indebted to Dr. R. L. Garman of the Chemistry Department of Washington Square College for the microphotometer curves.

[9] K. Clusius, Zeits. f. physik. Chemie **B3**, 41 (1929).

[10] Below the transition point, $T=98°K$, the heat capacity contributions due to a frequency of about 200 cm^{-1}, taken as a mean lattice frequency, give good agreement, when combined with the contributions of the transverse 72 cm^{-1}, with C_v values obtained from C_p data of Clusius by means of the Nernst-Lindemann C_p-C_v formula.

On the Calculation of Intensity Factors for the Powder Method of X-Ray Crystal Analysis

F. C. BLAKE, *Mendenhall Laboratory of Physics, Ohio State University*

(Received March 3, 1934)

In the July issue of *Reviews of Modern Physics* the writer has surveyed the literature as to intensity factors for the several methods of x-ray analysis. In this survey it was shown that both the atomic form factor F and the temperature factor e^{-M} properly enter into the so-called structure factor. Using the terminology of this survey one can distinguish then between the "regular" structure factor S, given by Eq. (51) of the survey, and what is here called the "reduced" structure factor S_0, given by SFe^{-M}. It is highly important both to the pure physicist and to the industrial physicist to be able properly to get S_0 out of S. How this is done is illustrated in this paper both for wurtzite or α-ZnS and for sphalerite or β-ZnS. It was shown in the survey that the reason why it is necessary to operate with the reduced structure factor is on account of the phase differences between the waves diffracted by the several electrons of the *same* atom, reduced further by the levelling effect of temperature. How these levelling effects are carried out is here shown. On account of the good observational material available for wurtzite the calculations for this are shown first.

I. Calculation of Regular Structure Factor

WURTZITE is known[1] to be a hexagonal crystal having $a=3.84$A with axial ratio $2(\frac{2}{3})^{\frac{1}{2}}$, giving $c=6.28$A. Its space group is C_{6v}^4. Ewald and Hermann[2] give the literature published on wurtzite. I have taken the results of Fuller[3] as among the best, and the comparison between theory and experiment is made with his results alone. I illustrate first the calculation of the regular structure factor and later that of the reduced factor. Such calculations are much more easily made by operating with the revolving vector than by dealing with sines and cosines. On the other hand, the method of revolving vectors has no advantages for those crystals where symmetry considerations make either the sines or the cosines drop out everywhere. All basal pinacoids except those of even index are of zero intensity hence the first line on a powder photograph for wurtzite is due to face $10\bar{1}0$. Wurtzite has two molecules of ZnS per unit cell, the atoms of zinc being located at the positions $\frac{1}{3}\frac{\bar{1}}{3}0$, $\frac{\bar{1}}{3}\frac{1}{3}\frac{1}{2}$ and of sulphur at positions $\frac{1}{3}\frac{\bar{1}}{3}\frac{3}{8}$, $\frac{\bar{1}}{3}\frac{1}{3}\frac{\bar{1}}{8}$.

In the Survey,[4] page 186, the regular structure factor is shown to be

$$S=\sum_r Z_r e^{2\pi i(x_r h+y_r k+z_r l)}, \qquad (1)$$

where $x_r y_r z_r$ are the coordinates of the rth atom and hkl are the indices, here Bravais-Miller. In considering the face $10\bar{1}0$ (usually written $10\cdot 0$, where $h+k+i=0$) one can write in a sort of shorthand $S=30[\frac{1}{3}, \frac{\bar{1}}{3}]+16[\frac{1}{3}, \frac{\bar{1}}{3}]=-46$. Draw two concentric circles, one of radius 16, the atomic number of sulphur, the other of radius 30, the atomic number of zinc. Thinking in terms of the revolving vector we draw two vectors for zinc at positions 120° and 240° away from the positive X-axis. Similarly, we draw two vectors in exactly the same angular positions for sulphur. The resultant of the two zinc vectors is a single vector of magnitude 30 lying along the negative X-axis and that of the two sulphur vectors is a single vector of magnitude 16 lying in the same position as the zinc resultant. Hence the regular structure factor is $S=-30-16=-46$ and $|S|^2=2116$. Because of the influences of the atomic form factor and the temperature factor in reducing the structure factor and different amounts for different atoms I have found it con-

[1] Goldschmidt, *Geochemische Verteilungsgesetze der Elements, VIII;* see reference 2.

[2] Ewald and Hermann, *Strukturbericht*, p. 128, 1913–1928.

[3] M. L. Fuller, Phil. Mag. **8**, 658 (1929).

[4] F. C. Blake, Rev. Mod. Phys. **5**, 169 (1933). This article will be referred to as "Survey" throughout paper.

venient in Tables I and II to indicate the regular structure factor S as the sum of two separate quantities rather than as a single quantity. Of course, when the resultant vectors due to the zinc atoms and to the sulphur atoms separately do not lie along the same direction it is necessary to indicate S as a complex number.

Again consider face 0002 (00·2) due to the basal pinacoids. Here Eq. (1) gives $S=60-32i$ at once, for the two zinc vectors lie along the positive X-axis and the two sulphur vectors along the negative Y-axis. In Fig. 1 it is convenient in finding the resultant vector for the several faces there shown to draw two concentric circles, one of radius 30, the other of radius 16, or integral multiples of these numbers, hence in the figure corresponding circles look alike but may have different radii.

Face $10\bar{1}1$ (10·1) is typical of the more complicated patterns of revolving vectors. In my shorthand notation I write

$$S=30[\tfrac{1}{3},\ \tfrac{1}{6}]+16[\tfrac{\bar{7}}{24},\ \tfrac{\overline{11}}{24}]. \qquad (2)$$

The reader can understand this in the following way. Eq. (1) gives

$$\begin{aligned} S=&30[e^{2\pi i(1/3\cdot 1+\bar{1}/3\cdot 0+0\cdot 1)}\\ &+e^{2\pi i(\bar{1}/3\cdot 1+1/3\cdot 0+1/2\cdot 1)}]\\ &+16[e^{2\pi i(1/3\cdot 1+\bar{1}/3\cdot 0+3/8\cdot 1)}\\ &+e^{2\pi i(\bar{1}/3\cdot 1+1/3\cdot 0+\bar{1}/8\cdot 1)}]\\ =&30[e^{2\pi i(1/3)}+e^{2\pi i(1/6)}]\\ &+16[e^{2\pi i(17/24)}+e^{2\pi i(\overline{11}/24)}] \qquad (3) \end{aligned}$$

which may be shortened to the form given by (2) for the reason that the coefficient of $2\pi i$ in the exponents of the Naperian base indicates the direction of the amplitude vector. Thus in (2) the figures $\frac{1}{3}$ and $\frac{1}{6}$ state that the two zinc vectors lie along directions 120° and 60° away from the positive X-axis, these figures being in each case $\frac{1}{3}$ and $\frac{1}{6}$ of a complete rotation (360°). For the two sulphur vectors, on the other hand, we have rotations $\frac{1}{24}\frac{7}{}(=\frac{\bar{7}}{24})$ and $\frac{\overline{11}}{24}$, that is, directions −105° and −165°. Drawing the vectors indicated in the third figure of Fig. 1, the resultant of the two zinc vectors gives a vector 51.96 (=52) along the positive Y-axis. The resultant of the two sulphur vectors gives a vector 27.7 along the direction −135°. This has the two components −19.6 and $-19.6i$. The final resultant, indicated in the figure, may accordingly be written $S=52i-19.6(1+i)$. There is nothing gained by writing this $32.4i-19.6$ except for getting $|S|^2$ in column 6 of Table I, written S^2. For in getting the reduced structure factor S_0 one must take the resultant amplitude 52 for the zinc atoms and multiply it by Fe^{-M} for zinc; again the resultant sulphur amplitude 27.7 must be multiplied by Fe^{-M} for sulphur and this function Fe^{-M} is a function of the atomic number, directly in F and indirectly through the atomic weight in M. The reader should now be able to check for himself the resultant amplitude vectors in the other figures of Fig. 1.

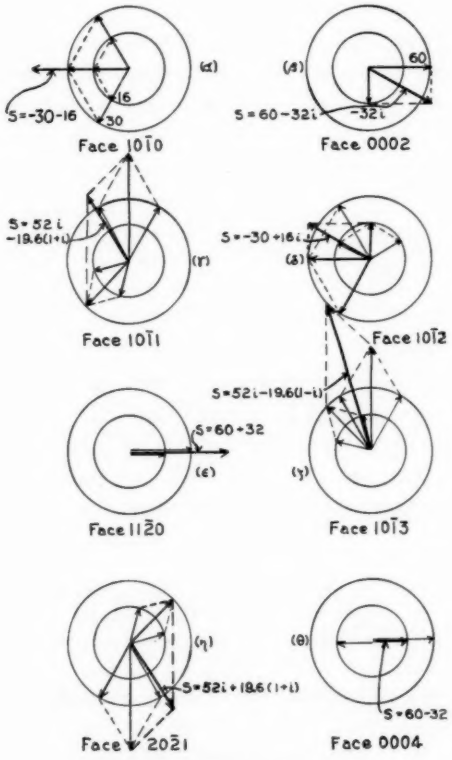

FIG. 1. Wurtzite, α-ZnS.

Going now to sphalerite or β-ZnS, it is known[5] to be face-centered cubic of the diamond type containing four molecules, a being 5.43A. Its space group is T_d^2. The zinc atoms are at positions 000, $\frac{1}{2}\frac{1}{2}0$, $\frac{1}{2}0\frac{1}{2}$, $0\frac{1}{2}\frac{1}{2}$, and the sulphur atoms at positions $\frac{1}{4}\frac{1}{4}\frac{1}{4}$, $\frac{1}{4}\frac{\bar{1}}{4}\frac{\bar{1}}{4}$, $\frac{\bar{1}}{4}\frac{1}{4}\frac{\bar{1}}{4}$, $\frac{\bar{1}}{4}\frac{\bar{1}}{4}\frac{1}{4}$, or *vice versa*. For all faces whose regular structure factor

[5] Reference 2, pp. 77 and 127; also reference 1, p. 28.

TABLE I. *Wurtzite, α-ZnS.*

Face	θ	$\sin\theta$	S	S_0	S^2	S_0^2	S_0^2/S^2	n	Φ	A	I (A omitted)	I (A included)	I (obs.) (Fuller)	I (calc.) (Fuller)
10·0	6−7.7	0.1068	$-30-16$	-36.2	2116	1310	62.0	12	87.1	1.00	97.3	95.6	80	85.5
00·2	6−30.1	.1132	$60-32i$	$47.3-23.5i$	4624	2793	60.3	2	76.3	1.01	30.3	30.0	32	52
10·1	6−56.3	.1208	$52.0i-19.6(1+i)$	$26.0i-14.0$	1434	872	60.8	24	67.2	1.02	100.0	100.0	76	71.3
10·2	8−57.1	.1556	$-30+16i$	$-21.0+10.0i$	1156	541	46.8	24	37.5	1.07	34.0	36.4	20	36.7
11·0	10−39.3	.1849	$60+32$	56.5	8464	3192	37.8	12	27.8	1.13	74.4	84.1	96	93.2
10·3	11−34.3	.2006	$52.0i-19.6(1-i)$	$42.5i-10.3$	5511	1912	34.7	24	23.4	1.16	75.0	87.0	100	100.0
20·0	12−19.7	.2135	$-30-16$	26.1	2116	681	32.2	12	20.3	1.18	11.6	13.7	(?)	16.5
11·2	12−31.3	.2168	$60-32i$	$35.4-16.0i$	4624	1508	32.6	12	19.9	1.19	25.2	29.9	34	70.6
20·1	12−45.6	.2209	$-52.0i+19.6(1+i)$	$-20.3i+9.8$	2165	508	23.5	24	19.1	1.20	16.2	19.5	6	17.3
00·4	13−5.3	.2265	$60-32$	18.6	784	346	44.2	2	18.0	1.21	.87	1.05		
20·2	13−59.1	.2417	$-30+16i$	$-16+3.6i$	1156	269	23.3	24	16.0	1.23	7.22	9.77	(?)	12.9
10·4	14−29.9	.2504	$-30+16$	8.91	196	79	40.3	24	14.3	1.25	1.98	2.48		
20·3	15−49.9	.2728	$-52.0i-19.6(1-i)$	$-34.3i+8.1$	5511	1242	22.5	24	11.9	1.31	24.8	32.5	22	48.4
12·0	16−24.4	.2824	$-30-16$	-21.1	2116	446	21.0	12	11.1	1.34	4.15	5.56	4	36.3
12·1	16−44.5	.2881	$-52.0i+19.6(1+i)$	$-17.6i+7.6$	1434	368	25.6	24	10.6	1.35	6.54	8.83	4	18.5
11·4	16−59.9	.2924	$60-32$	16.5	784	272	34.8	12	10.3	1.36	2.35	3.20		
10·5	17−36.6	.3025	$52.0i+19.6(1+i)$	$31.3i+7.2$	5511	1033	18.8	24	9.5	1.39	16.4	22.9	16	57.7
12·2	17−42.6	.3043	$-30+16i$	$-13.8+5.9i$	1156	225	19.5	24	9.4	1.40	3.55	4.97		
20·4	18−8.0	.3112	$-30+16$	-8.0	196	64	32.6	24	9.0	1.41	.97	1.36		
30·0	18−40.7	.3203	$60+32$	37.8	8464	1429	16.8	12	8.4	1.44	10.07	14.5	8	25.8
12·3	19−14.6	.3296	$-52.0i+19.6(1-i)$	$-29.2i+6.6$	5511	895	16.2	24	7.9	1.46	11.8	17.3	27	62.1
00·6, 30·2	19−51.4	.3397	$60\pm32i$	$25.3\pm10.5i$	4624	750	16.2	2, 24	7.3	1.50	9.9	14.9	(?)	4.0
20·5	20−46.3	.3546	$-52.0i-19.6(1-i)$	$-15.0i-6.0$	1434	261	18.2	24	6.6	1.54	2.90	4.47	4	33.8
10·6	20−51.5	.3561	$-30-16i$	$-12.1-4.9i$	1156	170	14.6	24	6.5	1.55	1.85	2.87		
12·4	21−13.4	.3620	$-30+16$	-7.1	196	50	25.5	24	6.3	1.56	0.53	0.82		
22·0	21−42.2	.3698	$60+32$	32.7	8464	1070	12.6	12	6.0	1.59	5.38	8.56	2	16.1
13·0	22−38.2	.3849	$-30-16$	-15.6	2116	243	11.5	12	5.5	1.65	1.12	1.85		
11·6, 22·2	22−45.1	.3867	$60-32i$	$22.3-8.7i$	4624	573	12.4	12, 12	5.4	1.66	5.18	8.61	8	16.9
13·1	22−53.7	.3890	$52.0i-19.6(1+i)$	$13.9i-5.3$	1434	221	15.4	24	5.3	1.67	1.96	3.28		
30·8, 33·0	33−41.4	.5547	$60+32$	18.9	8464	357	4.2	24, 12	2.3	2.39	2.10	4.94		
60·0	39−49.7	.6405	$60+32$	14.5	8464	210	2.5	12	1.7	2.87	0.30	0.84		
36·0	57−55.1	.8473	$60+32$	7.5	8464	56	0.66	12	1.5	4.36	0.07	0.30		
00·16	64−56.0	.9058	$60+32$	6.4	8464	41	0.48	2	2.0	4.93	0.01	0.05		
36·8, 90·0, 30·16	73−53.8	.9608	$60+32$	5.1	8464	26	0.31	24, 12, 24	3.4	5.55	0.38	2.07		
80·8	75−10.0	.9667	$60+32$	4.9	8464	24	0.28	24	3.6	5.62	0.14	0.81		
33·14, 90·2	75−20.0	.9674	$60\pm32i$	$4.3\pm0.7i$	4624	19	0.41	12, 24	3.7	5.63	0.18	1.00		
28·0	78−4.0	.9784	$60+32$	4.7	8464	22	0.26	12	4.6	5.77	0.09	0.50		
28·2, 17·10	80−2.0	.9849	$60\pm32i$	$4.0\pm0.6i$	4624	16	0.35	24, 24	5.6	5.86	0.31	1.78		

is other than zero there are only four possibilities, 120 ± 64 or $120\pm64i$. Consider the first face to give a reflection on the powder photograph, *viz.*, 111. Draw two concentric circles of radii $120(=4\times30)$ and $64(=4\times16)$. (See Fig. 2.) Eq. (1) gives

$$S=30[e^{2\pi i(0\cdot1+0\cdot1+0\cdot1)}+e^{2\pi i(\frac{1}{2}\cdot1+\frac{1}{2}\cdot1+0\cdot1)}+e^{2\pi i(\frac{1}{2}\cdot1+0\cdot1+\frac{1}{2}\cdot1)}+e^{2\pi i(0\cdot1+\frac{1}{2}\cdot1+\frac{1}{2}\cdot1)}]+16[e^{2\pi i(\frac{1}{4}\cdot1+\frac{1}{4}\cdot1+\frac{1}{4}\cdot1)}+e^{2\pi i(\frac{1}{4}\cdot1+\frac{\bar{1}}{4}\cdot1+\frac{\bar{1}}{4}\cdot1)}+e^{2\pi i(\frac{\bar{1}}{4}\cdot1+\frac{1}{4}\cdot1+\frac{\bar{1}}{4}\cdot1)}+e^{2\pi i(\frac{\bar{1}}{4}\cdot1+\frac{1}{4}\cdot1+\frac{\bar{1}}{4}\cdot1)}], \quad (4)$$

which in my abbreviated notation may be written

$$30[0,\ 0,\ 0,\ 0]+16[\tfrac{1}{4},\ \tfrac{1}{4},\ \tfrac{1}{4},\ \tfrac{1}{4}]. \quad (5)$$

Eq. (5) shows that the four zinc atoms give amplitude vectors that superpose along the positive X-axis and the four sulphur atoms give amplitude vectors that superpose along the

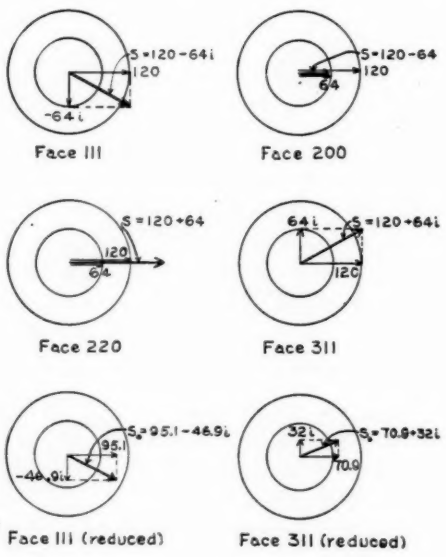

FIG. 2. Sphalerite, β-ZnS.

TABLE II. *Sphalerite, β-ZnS.*

Face	θ	$\sin\theta$	S	S_0	S^2	S_0^2	S_0^2/S^2	n	Φ	A	I (calc.) A (omitted)	I (calc.) (A incl.)	I (obs.)
111	6−31.0	0.1135	$120-64i$	$95.1-46.9i$	18496	11240	60.8	8	76.3	1.00	100.0	100.0	100
200	7−30.8	.1308	$120-64$	48.6	3136	2360	75.2	6	57.0	1.02	11.8	12.0	—
220	10−39.4	.1849	$120+64$	106.9	33856	11425	33.8	12	27.8	1.13	56.3	63.7	52.8
311	12−31.4	.2169	$120+64i$	$70.9+32i$	18496	6051	32.7	24	19.9	1.19	42.1	50.1	48.4
222	13−5.4	.2265	$120-64$	36.4	3136	1325	42.3	8	18.0	1.21	2.72	3.29	—
400	15−9.6	.2615	$120+64$	90.3	33856	8154	24.0	6	13.0	1.27	9.27	11.8	5.3
331	16−33.5	.2850	$120-64i$	$58.9-25.1i$	18496	4100	22.2	24	10.9	1.34	15.6	21.0	16.3
420	17−0.0	.2924	$120-64$	32.3	3136	1044	33.3	24	10.3	1.36	3.76	5.12	—
422	18−40.8	.3203	$120+64$	75.9	33856	5761	17.0	24	8.4	1.44	17.0	24.4	18.5
511, 333	19−51.6	.3397	$120\pm64i$	$50.8\pm20.6i$	18496	3004	16.2	24, 8	7.3	1.50	10.2	15.3	8.8
440	21−42.3	.3698	$120+64$	65.6	33856	4290	12.7	12	6.0	1.59	4.50	7.16	5.3
531	22−45.4	.3868	$120+64i$	$44.5-17.5i$	18496	2286	12.4	48	5.4	1.66	8.64	14.3	4.4
620	24−25.4	.4135	$120+64$	57.4	33856	3300	9.7	24	4.6	1.74	5.31	9.25	3.2
533	25−22.1	.4287	$120-64i$	$41.0-15.6i$	18496	1924	10.4	24	4.2	1.80	2.83	5.09	
444	26−56.0	.4530	$120+64$	51.0	33856	2601	7.7	8	3.70	1.90	1.12	2.13	
551, 711	27−50.0	.4669	$120\pm64i$	$36.5\pm12.9i$	18496	1498	8.1	24, 24	3.40	1.95	3.57	6.96	
642	29−17.5	.4892	$120+64$	46.7	33856	2181	6.4	48	3.0	2.02	4.58	9.25	
553, 731	30−8.7	.5022	$120\pm64i$	$32.9\pm11.3i$	18496	1310	7.1	24, 48	2.83	2.12	3.89	8.25	
800	31−32.1	.5230	$120+64$	41.8	33856	1750	5.2	6	2.68	2.20	0.41	0.90	
822, 660	32−49.7	.5421	$120+64$	38.6	33856	1490	4.4	24, 12	2.40	2.32	1.88	4.36	
840	35−47.2	.5848	$120+64$	34.5	33856	1190	3.5	24	2.00	2.54	0.83	2.11	
664	37−49.7	.6133	$120+64$	31.5	33856	993	2.9	24	1.80	2.72	0.63	1.71	
844	39−50.1	.6406	$120+64$	29.6	33856	874	2.6	24	1.63	2.87	0.50	1.43	
862, 1020	41−45.4	.6660	$120+64$	27.0	33856	729	2.2	48, 24	1.50	2.97	1.15	3.41	
1042	45−44.4	.7162	$120+64$	23.1	33856	534	1.6	48	1.41	3.37	0.53	1.79	
880	47−42.1	.7397	$120+64$	21.5	33856	463	1.4	12	1.38	3.52	0.11	0.39	
866, 1060	49−41.7	.7624	$120+64$	19.7	33856	388	1.1	24, 24	1.37	3.70	0.37	1.37	
884, 1200	51−40.6	.7845	$120+64$	18.6	33856	346	1.02	24, 6	1.38	3.85	0.21	0.81	
1240	55−47.3	.8270	$120+64$	16.1	33856	259	0.76	24	1.46	4.19	0.13	0.55	
888	64−57.7	.9059	$120+64$	12.2	33856	149	0.44	8	1.98	4.93	0.03	0.17	
1086, 1420	67−36.2	.9246	$120+64$	11.4	33856	130	0.38	48, 24	2.31	5.14	0.32	1.62	
1280	70−32.5	.9429	$120+64$	10.8	33856	117	0.35	24	2.62	5.38	0.11	0.59	
997, 1193	71−44.6	.9497	$120-64i$	$8.98-1.51i$	18496	83	0.45	24, 48	2.85	5.43	0.25	1.36	
1266, 10104, 1442	73−55.0	.9609	$120+64$	10.1	33856	102	0.30	24, 24, 48	3.32	5.55	0.48	2.67	
1177, 1355, 1371	75−21.0	.9675	$120\pm64i$	$8.49+1.38i$	18496	74	0.40	24, 24, 48	3.70	5.63	0.38	2.14	
1284	78−6.0	.9785	$120+64$	9.5	33856	90	0.27	48	4.59	5.77	0.29	1.67	
1195, 1373, 1511	80−4.5	.9850	$120\pm64i$	$7.98+1.25i$	18496	66	0.36	48, 48, 24	5.58	5.86	0.64	3.77	
1088	80−49.0	.9872	$120+64$	9.2	33856	84	0.25	24	6.20	5.88	0.18	1.06	
1460	84−45.5	.9958	$120+64$	8.9	33856	80	0.24	24	11.00	6.01	0.31	1.86	

negative Y-axis, hence the resultant vector is $S=120-64i$ and $|S|^2$, designated as S^2 in column 6 of Table II, becomes $120^2+64^2=18496$. The reader can readily check the vector diagrams for the other figures of Fig. 2, face 200 giving $S=30[0,\ 0,\ 0,\ 0]+16[\frac{1}{2},\ \frac{1}{2},\ \frac{1}{2},\ \frac{1}{2}]=120-64$, face 220 giving $S=30[0,\ 0,\ 0,\ 0]+16[0,\ 0,\ 0,\ 0]=120+64$, and face 311 giving $S=30[0,\ 0,\ 0,\ 0]+16[\frac{1}{4},\ \frac{1}{4},\ \frac{1}{4},\ \frac{1}{4}]=120+64i$. Thus all possibilities are covered in these first four faces.

II. CALCULATION OF REDUCED STRUCTURE FACTOR

In the Survey, page 189, Fig. 26, there is shown plotted the atomic form factor for all the atoms for which the Thomas-Fermi distribution of electrons is justifiable. It is there (page 190) stated that probably this distribution holds for all atoms of atomic number greater than 23. Since for compounds the diffraction effects due to heavy atoms outweigh by far those due to light atoms, with zinc having atomic number 30 and sulphur 16 one is safe in saying that for zinc sulphide the Thomas-Fermi distribution holds, hence Fig. 26 of the Survey applies. That figure is here reproduced as Fig. 2a.

Consider now face $10\bar{1}0$ for wurtzite. Using λ for molybdenum $K\alpha$-rays as 0.710A we get $\sin\theta/\lambda$ for this face to be 0.1504 where the factor 10^8 is balanced out in Fig. 2a as it is in the Survey, Fig. 26, on account of its reciprocal being implied in the value of a. Now the "ground-length" a (Survey, page 189) for zinc is

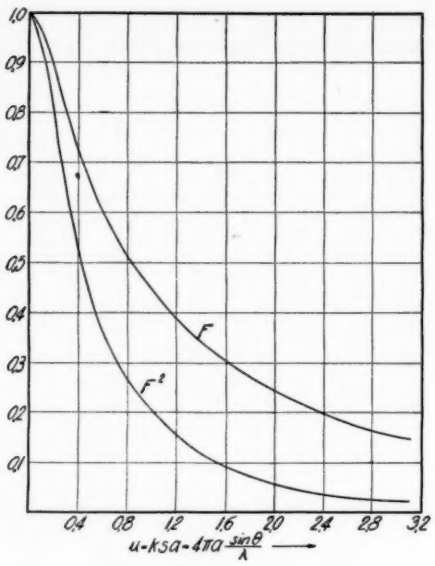

FIG. 2a.

$a=0.466/30^{\frac{1}{2}}=0.1499$A while that for sulphur is $a=0.466/16^{\frac{1}{2}}=0.1850$A. Hence the value of the abscissa u in Fig. 2a is

$$\left.\begin{aligned} u_{Zn}&=4\pi \sin\theta/\lambda\cdot a_{Zn}=2.653 \sin\theta \\ \text{while}\quad u_S&=4\pi \sin\theta/\lambda\cdot a_S =3.274 \sin\theta \end{aligned}\right\}. \quad (6)$$

Eq. (6) gives for face $10\bar{1}0$ $u_{Zn}=0.2835$ and $u_S=0.3498$. Reading off from Fig. 2a we get $F_{Zn}=0.815$ while $F_S=0.770$. Thus if there were no effect due to temperature the atomic form factor would reduce our value of S from $-30-16$ to $-30\cdot 0.815-16\cdot 0.770=-36.8$.

Using Debye's formula for the temperature effect (Survey Eq. (22)) we get

$$M=6h^2/mk\Theta\cdot\sin^2\theta/\lambda^2\{\phi(x)/x+\tfrac{1}{4}\}. \quad (7)$$

As stated by Professor Debye, this formula holds for atoms of a single kind only. However, I have used it as if it held for compounds, such as zinc sulphide. In Eq. (7) the fact that the mass of the atom appears in the denominator means that M is larger for sulphur than for zinc, and this means that the influence of temperature on the diffraction due to the sulphur atoms is more dissipant than on that due to the zinc atoms, a thing which surely must be in keeping with the physics of the situation, at least in large part. But this would take us back rather to the point of view of Debye's earlier papers, previous to the improvement made by Born and Karman (Survey, page 175). Hence it is discussed again after the comparison is made between calculation and observation in the case of wurtzite (see below).

I have taken Θ for zinc sulphide to be 325° absolute and T (room temperature) to be 22°C $=295°$ absolute, giving x in Eq. (7) to be 1.102. Thus M for zinc is evaluated as

$$M_{Zn}=\frac{6\cdot(6.55\times10^{-27})^2}{65.38\cdot1.649\times10^{-24}\cdot1.371\times10^{-16}}\times\left\{\frac{0.758}{1.102}+\tfrac{1}{4}\right\}\frac{\sin^2\theta}{\lambda^2}, \quad (8)$$

which for molybdenum $K\alpha$-rays becomes $M_{Zn}=0.998\sin^2\theta$. Substituting the atomic weight (32.06) for sulphur for that of zinc we get $M_S=2.030\sin^2\theta$. In Eq. (8) the factor 0.758 is $\phi(x)$ for $x=1.102$, interpolated from Survey, Table I. Thus for face $10\bar{1}0$ e^{-M} for zinc is 0.989 while that for sulphur is 0.977. Thus $(Fe^{-M})_{Zn}=0.806$ and $(Fe^{-M})_S=0.752$, giving $S_0=SFe^{-M}=-30\cdot0.806-16\cdot0.752=-36.2$ instead of -36.8, obtained when the temperature effect is ignored, showing, as is well known, that the diffusion or dissipance of the lines on a powder photograph due to temperature is small for $\sin\theta$ small. Further illustration of temperature calculations is unnecessary; one simply takes

$$M_{Zn}=0.998\sin^2\theta, \quad M_S=2.030\sin^2\theta, \quad (9)$$

looks up e^{-M} in a table and makes the calculations as above.

However, I deem it worth while to illustrate for face $10\bar{1}1$ how the factor Fe^{-M} reduces S from the value $52.0i-19.6(1+i)$ to $26.0i-14.0$. We find for this face $M_{Zn}=0.01457$ while $M_S=0.02965$, giving e^{-M} for zinc to be 0.986 and e^{-M} for sulphur to be 0.970. But u for zinc is found from (6) to be 0.3208 and for sulphur to be 0.3958, giving $F_{Zn}=0.780$ and $F_S=0.735$. Now it is obvious from Fig. 1 (γ) that it makes no difference whether I reduce each zinc component by multiplying it by $0.780\cdot0.986(=0.769)$ and each sulphur component by $0.735\cdot0.970$ $(=0.713)$ and then take resultants or whether I apply these figures respectively to the resultants

already taken. Hence we get S_0 for face $10\bar{1}1$ to be

$$52i\cdot 0.769-19.6(1+i)\cdot 0.713$$
$$=40.0i-14.0(1+i)=26.0i-14.0.$$

The reader now sees how the reduced structure factor is obtained from the regular structure factor and can readily check for himself the values of S and S_0 in Table I for wurtzite. The method is identical for sphalerite. I happen to have made the calculations in a somewhat different way than for wurtzite. Using the Bragg law, $n\lambda=2d\sin\theta$ and remembering that $d=a/(h^2+k^2+l^2)^{\frac{1}{2}}=a/r$, say, we get $u_1=4\pi a_1\sin\theta/\lambda=4\pi a_1 r/2a$, where a_1 is the ground length for zinc and a is the edge of the cubic lattice. Calling u_2 the corresponding u for sulphur we get $u_2=4\pi a_2 r/2a$. One can calculate $2\pi a_1/a$ and $2\pi a_2/a$ once for all, which give the u's for each face when multiplied by its corresponding r. I have ignored for the time being the possibility that the elastic spectrum for hexagonal crystals may not necessarily be the same as for cubic crystals and have used (9) both for wurtzite and sphalerite. We get then for face 111 of sphalerite $u_1=0.3004$ and $u_2=0.3708$, giving $F_1=0.803$ and $F_2=0.754$. Now $M_1=0.01286$ and $M_2=0.02615$, giving $e^{-M_1}=0.987$ and $e^{-M_2}=0.973$. Thus $F_1e^{-M_1}=0.792$ and $F_2e^{-M_2}=0.733$. Whence

$$S_0=120\cdot 0.792-64i\cdot 0.733=95.1-46.9i.$$

The reduced structure factor for the other faces follow equally easily. I have collected into tables, Tables III and IV, the quantities that are useful in getting the reduced structure factor after the regular structure has been obtained, both for wurtzite and sphalerite.

I have also inserted in Tables I and II not only S and S_0 but also S^2 and S_0^2, written without the absolute value signs and then S_0^2/S^2. It is interesting to see how this fraction bobs up and down both for wurtzite and for sphalerite when plotted against $\sin\theta$, as shown in Figs. 3 and 4. It should be stated that in Tables I and III no lines are omitted through face 13·1, but beyond

TABLE III. *Wurtzite.*

Face	Sin θ	U_1	F_1	U_2	F_2	M_1	e^{-M_1}	M_2	e^{-M_2}	$F_1e^{-M_1}$	F_2e^{-M}
10·0	0.1068	0.284	0.815	0.350	0.770	0.0114	0.989	0.0232	0.977	0.806	0.752
00·2	.1132	.300	.803	.371	.754	.0128	.987	.0261	.974	.792	.735
10·1	.1208	.321	.780	.396	.735	.0146	.986	.0300	.970	.768	.713
10·2	.1556	.413	.720	.509	.657	.0242	.975	.0491	.951	.702	.625
11·0	.1849	.491	.669	.605	.595	.0341	.966	.0694	.933	.646	.555
10·3	.2006	.536	.646	.662	.570	.0408	.960	.0831	.920	.620	.524
20·0	.2135	.566	.626	.699	.555	.0455	.956	.0925	.912	.598	.506
11·2	.2168	.575	.619	.710	.550	.0469	.954	.0955	.909	.590	.500
20·1	.2209	.586	.609	.723	.539	.0487	.952	.0991	.906	.579	.488
00·4	.2265	.601	.599	.741	.536	.0512	.950	.1040	.904	.569	.485
20·2	.2417	.655	.573	.810	.505	.0611	.940	.1242	.883	.535	.445
10·4	.2504	.664	.569	.819	.503	.0626	.939	.1274	.880	.534	.444
20·3	.2728	.724	.544	.893	.477	.0741	.929	.1507	.860	.505	.410
12·0	.2824	.751	.533	.926	.463	.0796	.924	.1619	.851	.493	.394
12·1	.2881	.765	.526	.943	.458	.0828	.921	.1685	.845	.484	.387
11·4	.2924	.776	.521	.957	.454	.0853	.918	.1736	.841	.478	.382
10·5	.3025	.803	.508	.991	.442	.0913	.913	.1857	.830	.464	.367
12·2	.3043	.808	.505	.997	.439	.0924	.912	.1880	.829	.460	.364
20·4	.3112	.830	.500	1.024	.431	.0976	.907	.1983	.820	.454	.353
30·0	.3203	.851	.493	1.049	.426	.1024	.903	.2080	.812	.445	.346
12·3	.3296	.875	.485	1.080	.416	.1081	.897	.2193	.803	.435	.334
00·6 } 30·2 }	.3397	.901	.474	1.112	.406	.1152	.891	.2340	.791	.422	.321
20·5	.3546	.941	.459	1.162	.397	.1255	.882	.2551	.775	.405	.307
10·6	.3561	.945	.457	1.167	.395	.1266	.881	.2573	.773	.402	.306
12·4	.3620	.960	.452	1.185	.391	.1309	.877	.2660	.766	.396	.299
22·0	.3698	.980	.447	1.210	.384	.1364	.873	.2778	.758	.390	.291
13·0	.3849	1.021	.433	1.260	.373	.1479	.863	.3003	.741	.374	.276
11·6 } 22·2 }	.3867	1.026	.431	1.265	.370	.1493	.861	.3020	.738	.371	.273
13·1	.3890	1.033	.429	1.274	.369	.1510	.860	.3070	.736	.369	.271
30·8 } 33·0 }	.5547	1.470	.325	1.815	.267	.3071	.736	.6250	.535	.239	.143
60·0	.6405	1.696	.285	2.094	.230	.4085	.665	.8320	.435	.189	.100
36·0	.8473	2.248	.213	2.774	.167	.7165	.489	1.458	.233	.104	.039
00·16	.9058	2.400	.198	2.967	.155	.8184	.441	1.667	.189	.087	.029
36·8 } 90·0 } 30·16 }	.9608	2.548	.182	3.143	.145	.9212	.398	1.873	.154	.073	.022
80·8	.9667	2.563	.180	3.165	.144	.933	.394	1.897	.150	.071	.022
90·2 } 33·14 }	.9674	2.566	.180	3.167	.144	.934	.393	1.900	.150	.071	.022
28·0	.9784	2.590	.178	3.200	.142	.955	.385	1.988	.137	.069	.020
28·2 } 17·10 }	.9849	2.62	.175	3.22	.141	.968	.379	2.00	.135	.066	.019

TABLE IV. *Sphalerite.*

Face	Sin θ	U_1	F_1	U_2	F_2	M_1	e^{-M_1}	M_2	e^{-M_2}	$F_1e^{-M_1}$	F_2e^{-M}
111	0.1135	0.300	0.803	0.371	0.754	0.0129	0.987	0.0262	0.973	0.792	0.735
200	.1308	.339	.785	.428	.712	.0171	.982	.0347	.965	.771	.687
220	.1849	.491	.670	.606	.598	.0341	.965	.0694	.933	.643	.558
311	.2169	.575	.620	.710	.550	.0469	.953	.0955	.909	.591	.500
222	.2265	.601	.600	.742	.535	.0512	.950	.1043	.901	.570	.486
400	.2615	.694	.557	.856	.494	.0683	.934	.1390	.879	.521	.434
331	.2850	.756	.533	.933	.462	.0810	.922	.1647	.848	.491	.392
420	.2924	.776	.526	.957	.456	.0853	.918	.1736	.840	.483	.383
422	.3203	.850	.496	1.049	.426	.1014	.903	.2065	.813	.448	.346
511 } 333 }	.3397	.901	.475	1.112	.407	.1152	.892	.2343	.793	.423	.322
440	.3698	.981	.447	1.211	.385	.1366	.873	.2780	.758	.390	.292
531	.3868	1.026	.432	1.266	.371	.1493	.860	.3037	.739	.371	.274
620	.4135	1.097	.412	1.354	.350	.1707	.843	.3460	.707	.347	.247
533	.4187	1.111	.407	1.371	.345	.1748	.839	.3550	.701	.342	.243
444	.4530	1.202	.386	1.483	.323	.2048	.814	.417	.660	.314	.207
551 } 711 }	.4669	1.239	.378	1.529	.313	.2176	.804	.443	.643	.304	.201
642	.4892	1.298	.362	1.602	.301	.2390	.803	.486	.615	.291	.185
553 } 731 }	.5022	1.332	.353	1.644	.293	.2515	.777	.512	.599	.274	.176
800	.5230	1.388	.343	1.713	.284	.2730	.761	.555	.573	.261	.163
822 } 660 }	.5421	1.472	.325	1.816	.268	.2933	.747	.596	.550	.243	.147
840	.5848	1.551	.309	1.915	.256	.341	.710	.694	.499	.219	.128
664	.6133	1.627	.296	2.008	.241	.376	.686	.763	.466	.203	.112
844	.6406	1.661	.290	2.097	.230	.410	.664	.833	.435	.193	.100
862 } 1020 }	.6660	1.767	.275	2.181	.221	.443	.643	.900	.407	.177	.090
1042	.7162	1.900	.258	2.345	.204	.512	.599	1.040	.353	.154	.072
880	.7397	1.962	.250	2.422	.196	.546	.580	1.110	.330	.145	.065
866 } 1060 }	.7624	2.023	.240	2.496	.186	.580	.560	1.180	.307	.134	.057
884 } 1200 }	.7845	2.081	.233	2.569	.180	.614	.546	1.249	.287	.127	.052
1240	.8270	2.194	.220	2.708	.170	.683	.505	1.388	.249	.111	.0424
888	.9059	2.403	.195	2.966	.155	.819	.441	1.665	.189	.0860	.0293
1086 } 1420 }	.9246	2.453	.190	3.027	.151	.853	.426	1.733	.177	.0810	.0267
1280	.9429	2.502	.185	3.087	.149	.881	.414	1.805	.164	.0767	.0244
997 } 1193 }	.9497	2.520	.184	3.110	.147	.901	.406	1.830	.160	.0747	.0236
1266 } 10104 } 1442 }	.9609	2.549	.181	3.146	.145	.921	.398	1.875	.155	.0720	.0225
1177 } 1355 } 1371 }	.9675	2.567	.180	3.168	.144	.934	.392	1.900	.150	.0707	.0216
1284	.9785	2.596	.177	3.204	.142	.956	.384	1.941	.144	.0680	.0205
1195 } 1373 } 1511 }	.9850	2.613	.175	3.225	.141	.968	.380	1.970	.139	.0665	.0196
1088	.9872	2.619	.175	3.232	.141	.973	.379	1.978	.138	.0663	.0194
1460	.9958	2.642	.173	3.261	.140	.990	.372	2.010	.134	.0644	.0188

that only certain lines are inserted to see how matters go for large angles. Similarly in Tables II and IV there are no lines omitted as far as face 800, but beyond that only certain lines are recorded, for the reason just given. Perhaps the most interesting feature of Figs. 3 and 4 is the sharp variations of S_0^2/S^2 for faces having θ small: Up to the value of sin θ where omissions occur, *viz.*, 0.3890 for wurtzite and 0.5230 for sphalerite, in these figures successive points are joined by short straight lines. The peaked character shown in Fig. 3 for those faces having $L=4$ stands out very prominently, but unfortunately in Mr. Fuller's paper reflections from those faces are not recorded, presumably because they were too weak to observe as shown by the intensity calculations recorded in columns 12 and 13 of Table I. For sphalerite we find similar peaks for faces 200, 222 and 420, and again columns 12 and 13 show them to be relatively weak in intensity. Conversely in Fig. 3 negative peaks might be said to be present for faces 20·1 and 20·2, and again they appear weak, for Fuller has observed intensity only about one-third that (correctly) calculated for 20·1, and 20·2 was not recorded. Omitting the peaks in both figures one can draw approximately smooth curves through the other points which clearly reveal the way both intra-atomic phase differences and diffusion or scattering due to temperature pull the reflection intensities down for increasing θ.

It could, of course, be successfully argued that the reason these peaks occur in Figs. 3 and 4 is that the temperature factor as applied in this paper, known to be based upon a theory built

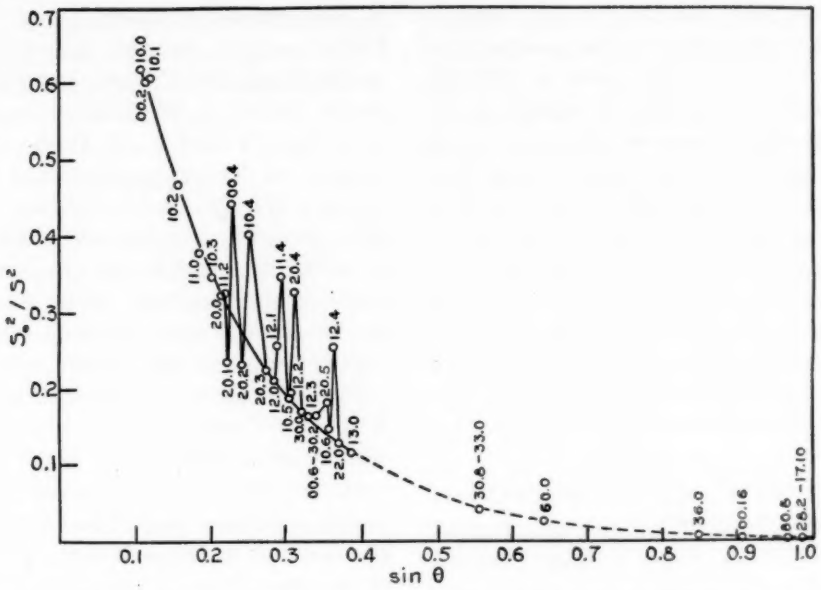

FIG. 3. Plot of [Reduced Structure Factor/Original Structure Factor]^2 *versus* sin θ for wurtzite or α-ZnS. ($\lambda = 0.710$A.)

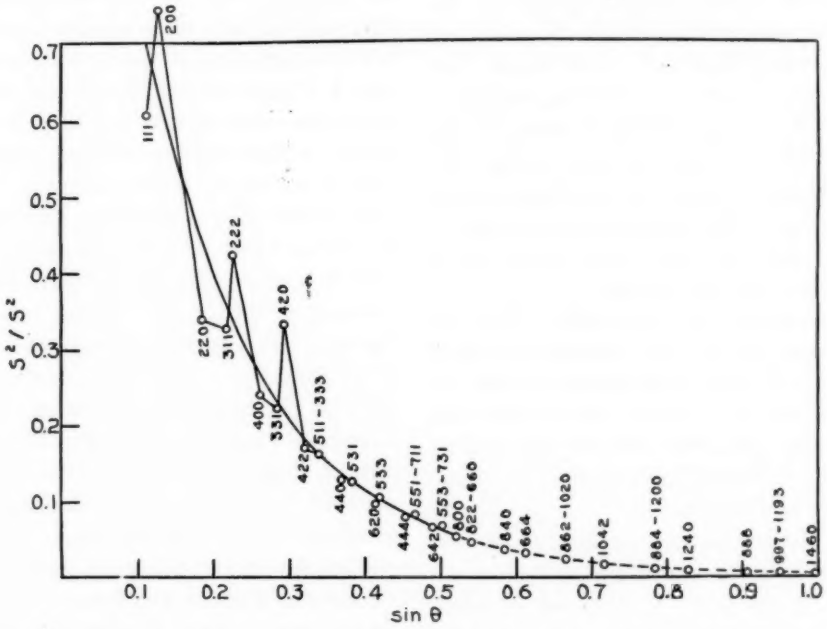

FIG. 4. Plot of [Reduced Structure Factor/Original Structure Factor]^2 *versus* sin θ for sphalerite or β-ZnS. ($\lambda = 0.710$A.)

upon one kind of atom only, is wrong and this in the long run may turn out to be the case. I have not had time, as yet, to try Waller's theory (Survey, page 176) of the temperature effect for crystals containing atoms of different kinds, but I mean to do this. It should be expected that the elastic constants of wurtzite and sphalerite are quite different. If the elastic data for these crystals are accurately known it will be interesting to see whether Waller's theory will make smooth curves out of Figs. 3 and 4.

Also recorded in Tables I and II are the values of the other factors occurring in the intensity formula (Survey, Eq. (73) or (74)); n is the form or multiplicity factor, Φ the combined Thomson-Lorentz factor, and A the absorption factor.

III. Comparison with Experiment

I have searched the literature for observations on sphalerite but have found nothing quantitative, Lehmann's[6] results, taken with copper rays, being qualitative. Accordingly I have run a powder sample of it, the crystal being kindly furnished me by Professor W. J. McCaughey. The results are shown in Table II. The last column shows the observed results, run on the photoelectric densitometer. Both a short exposure and a long exposure were made and allowance thereby made for overblackening of the first few lines, by the method given in the Survey (page 192). Just as was there (page 194) found, Table II shows about as good agreement with the calculated value, treating the absorption factor as constant, as with this value when allowance is made for absorption.

There is, of course, the possibility that the difference between theory and experiment, both in Table II and in the monograph, is due to inability properly to correct for extinction, especially primary extinction. Before this can be determined a special investigation must be made, and this is now under way.

There is good agreement found also for wurtzite where I have chosen Fuller's observations rather than those of Ulrich and Zachariasen,[7] for Fuller shows that they had as working material a mixture of wurtzite and sphalerite while he took special care to have no sphalerite in his sample. Column 14 of Table I gives Fuller's results for two samples which I have weighted equally. Column 15 gives his calculated results based on Wyckoff's formula. In column 12 of both Tables I and II the intensity is calculated on the assumption that the absorption factor is constant, while column 13 is calculated for both tables assuming the radius of the sample to be 0.2 mm and Θ, the characteristic temperature of zinc sulphide, to be 325°. This makes $\mu r = 3$ and the corresponding curve of Fig. 10, Survey, applies. The reader will readily admit the improvement of either column 12 or 13 over column 15 when compared with Fuller's observations, column 14. It should be stated that Fuller's observational material was obtained by visual inspection only. The writer desires to emphasize that the present status of our knowledge of the absorption factor as one important factor in the intensity formula can only be advanced by quantitative rather than qualitative measurements and recommends that more experimenters employ densitometers in their work. As shown by Tables I and II, the total effect on the absorption factor as θ is changed from 6° to 90° is 600 percent, and it would have been even more had I chosen the radius of the sample larger so as to use a curve of Fig. 10, Survey, below that used. Nevertheless it is difficult in Table I to say whether column 12 or column 13 is in better agreement with column 14. Certain remarks are in order. Any visual inspection method will underestimate the intensities of lines close in as compared with those farther away because of the greater general blackening close in. Hence it is *unproved* that line 10·3 is the strongest line on the powder photograph as Fuller gives it. The total range of θ in Fuller's observations was only 21° and in this range the change in A was only 66 percent, hence either column 12 or 13 appears almost equally good, when compared with column 14, though considering the qualitative character of the latter it certainly cannot be said that 12 is better than 13. We must await further experimental work.

It should be remarked, also, that, for zinc sulphide at least, when molybdenum rays are used even the A factor does not pull the intensity

[6] W. M. Lehmann, Zeits. f. Krist. **60**, 379 (1924); see also reference 1, p. 127.

[7] F. Ulrich and W. Zachariasen, Zeits. f. Krist. **62**, 260 (1925).

up sufficiently for values of θ near 90° to be able to observe such lines on a powder photograph. The matter could be helped by having a sample tube of larger radius. The case would be far different were copper rays used as shown by the Survey, page 195.

IV. Discussion

Certain readers will surely question the methods followed in this paper for getting the reduced structure factor when they recall that Debye's formula, Eq. (7), was worked out on the basis that the crystal lattice contained only one kind of atom. I have not attempted to insert a column in Tables I and II on the basis that I took an atom that would have an atomic number which is the mean between sulphur and zinc. Possibly an arithmetic mean, certainly a sort of center of gravity mean (preponderance of weighting in favor of the heavier atom), would give results very similar to columns 12 and 13. To do this would be rather futile until the observational material for compounds becomes quantitative. If and when it does, and if the other factors of the intensity formula are clinched experimentally as satisfactory, one could then throw light on the correct theory of the influence of temperature on the scattering power of different atoms. Certainly it seems reasonable that increasing temperature will cause lighter atoms to throw more of their energy, relatively, into the general blackening than heavier atoms will, leaving less in the Bragg reflection position—the calculations in this paper were made from this point of view.

The industrial x-ray analyst, desirous of improving his methods, is apt to balk at the labor involved in order to get the correct relative intensities on his powder photographs. Should he use the Debye-Scherrer-Hull method he will have to interpolate from Survey, Fig. 10, to get the correct A factor, depending upon his values of μ and r. Probably he will not be seriously in error, provided he is using $\lambda = 0.710$A, after he has calculated the first few lines on his photograph, to plot them and get the average value of S_0^2/S^2 (similar to Figs. 3 and 4) and extrapolate this value to larger values of θ. This paper lends support to the view that in general the scattering power of an atom, at least for atoms that do not interpenetrate, is independent of its physical state, for the scattering power of atoms obtained from gases seems to hold for crystals also.

In a recent paper Claassen and Burgers[8] have shown by means of x-rays the presence of a new intermetallic compound of zirconium and tungsten, *viz.* ZrW_2. It is interesting that the absorption factor covers a range of 4700 percent between the first, or 111, face and the last, or 844, face. They state that they chose the temperature factor such that there was agreement between theory and experiment at the beginning and end of the film, thereby obtaining a value of the coefficient B for the temperature factor $e^{-B}\sin^2\theta$, that is twice as great for the zirconium tungstide as for the value calculated for metallic tungsten, a result that is plausible considering the fact that ZrW_2 is lighter than W. This, of course, in no way precludes another factor or correction such as the extinction factor or the background factor being present, but is considered as absorbed into the temperature factor. Attempts are now being made to see whether the background factor (Survey, page 199) is confused in some way with the extinction correction factor, if present, in our experiments.

Coster, Knol and Prins[9] have shown for zinc blende both theoretically and experimentally that the structure factor for the octahedral (111) faces changes across the K-absorption limit for zinc. The K-absorption limit for zinc being at 1.281A, they show that for gold $L\alpha_2(\lambda = 1.285\text{A})$ the Zn and S scatter in phase with each other, while for gold $L\alpha_1(\lambda = 1.273\text{A})$ there is a phase difference of $10\frac{1}{2}$ degrees for the scattering from the zinc and sulphur atoms. Since we have used for zinc-blende x-rays from a molybdenum target, there can not be appreciable phase changes. Coster and Knol[10] have shown that the phase changes for reflections from iron and aluminum are not over $4\frac{1}{2}$ degrees, for $\lambda = 0.710$A for changes of $\sin\theta/\lambda$ from 0 to 1. Since the ratio of atomic numbers for iron and aluminum

[8] Claassen and Burgers, Zeits. f. Krist. **A86**, 100 (1933).

[9] Coster, Knol and Prins, Zeits. f. Physik **63**, 345 (1930). See also J. A. Prins, Zeits. f. Physik **47**, 479 (1928).

[10] Coster and Knol, Proc. Roy. Soc. **A139**, 459 (1933). See also Coster and Knol, Zeits. f. Physik **75**, 340 (1932).

is 2 to 1 and that for zinc and sulphur is somewhat less than this, we are safe in ignoring such possible phase differences for sphalerite.

V. Addenda

1. It is interesting to note that the density of wurtzite and of sphalerite is the same, *viz.* 4.01. For the volume of unit cell for wurtzite is $3.84^2 \cdot \sin 60° \cdot 6.28\text{A}^3 = 80.20\text{A}^3$, while the corresponding mass is $2(65.38+32.06)1.649\times10^{-24} = 321.36\times10^{-24}$ g per unit cell. The volume of unit cell for sphalerite is $(5.43\text{A})^3 = 160.1\text{A}^3$ while its mass is 642.72. Evidently if a for wurtzite is accurately 3.84A and $2(\frac{2}{3})^{\frac{1}{2}}$ is the correct axial ratio, the edge of the cube for sphalerite should be $(160.40)^{\frac{1}{3}} = 5.433\text{A}$. Fuller gives for the dimensions of the unit cell of wurtzite $a = 3.811 \pm 0.004\text{A}$, $c = 6.234 \pm 0.006\text{A}$, $c/a = 1.636$ instead of $1.6328 (= 1.633)$A. From these figures the volume per unit cell is 78.40A^3.

2. To get $\mu r = 3$ for ZnS we have $(N\lambda)_{Zn} = 30 \cdot 0.710 = 21.3$, $(N\lambda)_S = 16 \cdot 0.710 = 11.4$, giving $(\mu_e L)_k$[11] for zinc 119 and $(\mu_e L)_k$ for sulphur 19.9. Thus

$$\left(\frac{\mu}{\rho}\right)_{Zn} = \frac{30 \cdot 119}{65.38} = 54.7 \text{ and } \left(\frac{\mu}{\rho}\right)_S = \frac{16 \cdot 19.9}{32.06} = 9.94.$$

Therefore $$\left(\frac{\mu}{\rho}\right)_{ZnS} = \frac{65.38 \cdot 54.7 + 32.06 \cdot 9.94}{65.38 + 32.06}$$

$$= 38.0, \text{ giving } \mu = 152.$$

Now r was taken as 0.2 mm, hence $\mu r = 3$.

[11] For notation see Jönsson, Uppsala Dissertation, 1928.

Electron Diffraction by the Oxides of Nitrogen

LOUIS R. MAXWELL, V. M. MOSLEY AND LOLA S. DEMING, *Bureau of Chemistry and Soils, Washington, D. C.*

(Received April 16, 1934)

Electron diffraction has been obtained by the transmission of electrons (20–35 kv) through molecular beams of N_2O, NO_2, N_2O_4 and N_2O_5. The molecular structure determinations were made by using the complete electron scattering formula including the incoherent scattering. The results can be summarized as follows: (1) *Nitrous oxide;* for a linear model the separation of the end atoms was found to be 2.38 ± 0.05A in exact agreement with Wierl's measurement on this structure. Unfortunately it is impracticable to distinguish between models of the form N−O−N and N−N−O. (2) *Nitrogen dioxide;* no diffraction rings were observed which is to be expected if the molecule is triangular with the N−O distance 1.15 to 1.3A. (3) *Nitrogen tetroxide;* the presence of one diffraction ring at $(1/\lambda)\sin\theta/2=0.455\pm0.01$ lead to the conclusion that the N−N distance is 1.6 to 1.7A for the model O_2N-NO_2. No definite angular relationship between the two planes containing the NO_2 groups could be determined. (4) *Nitrogen pentoxide;* again only one diffraction ring was observed. It occurred at a slightly greater angle than for N_2O_4 giving $(1/\lambda)\sin\theta/2=0.474\pm0.004$. The symmetrical model $O_2N-O-NO_2$ with the N−O distance 1.3 to 1.4A gave a calculated interference pattern in best agreement with this result.

THE diffraction of electrons by gases has been used as a method for determining the structure of molecules.[1] This analysis involves the interference theory originally developed for coherent x-ray scattering with the inclusion of the atomic electron scattering amplitudes. The importance of the incoherent electron scattering has been determined theoretically by Morse[2] and later summarized by Bewilogua.[3] For the purpose of obtaining nuclear separations it is usually unnecessary to consider the incoherent scattering; however, in some instances it should be included. These considerations will be discussed in the present work and a treatment of the structure determinations of the nitrogen oxides will be undertaken.

The angular distribution of coherent electron scattering can be expressed in the following manner:[4]

$$I(x)\sim\sum_{i=1}^{n}\sum_{j=1}^{n}\psi_i\psi_j(\sin x_{ij})/x_{ij},$$

where $I(x)$ is the intensity of scattering at angle θ per unit intensity of the primary beam at unit distance from the scattering molecule, while $x_{ij}=4\pi l_{ij}(\sin\theta/2)/\lambda$. Recent workers[5] have simplified this expression to the extent of replacing the scattering amplitude $\psi_i=Z_i-F_i/(\sin\theta/2)^2$ by simply Z_i (atomic number), an approximation although justifiable in some cases cannot be generally applied as will be shown below. A more complete electron scattering formula can be written as follows:[6]

$$I(x)=\frac{k}{((\sin\theta/2)/\lambda)^4}\times\left[\sum_{i=1}^{n}\sum_{j=1}^{n}(Z_i-F_i)(Z_j-F_j)\frac{\sin x_{ij}}{x_{ij}}+\sum_{i=1}^{n}Z_iS(\nu_i)\right]$$

where $\nu_i=4\pi b_i(\sin\theta/2)/\lambda$ while b_i is expressed in Angstroms and represents the characteristic

[1] R. Wierl, Ann. d. Physik **8**, 521 (1931); **13**, 453 (1932); Hengstenberg and Brú, Anales, Soc. Espana. Fis. y Quim. **30**, 341 (1932); **31**, 115 (1933); L. O. Brockway and Linus Pauling, Proc. Nat. Acad. Sci. **19**, pp. 68 and 860 (1933); L. O. Brockway, ibid. **19**, 303 (1933); **19**, 868 (1933); S. B. Hendricks, Louis R. Maxwell, V. M. Mosley and M. E. Jefferson, J. Chem. Phys. **1**, 549 (1933); Ralph W. Dornte, J. Chem. Phys. **1**, 566 and 630 (1933); J. Am. Chem. Soc. **55**, 4126 (1933); H. Braune and S. Knoke, Zeits. f. physik. Chemie **B21**, 297 (1933).

[2] Ph. M. Morse, Phys. Zeits. **33**, 443 (1932).

[3] L. Bewilogua, Phys. Zeits. **33**, 688 (1932).

[4] Cf., J. Chem. Phys. **1**, 549 (1933).

[5] R. Wierl, Ann. d. Physik **13**, 453 (1932); L. O. Brockway and Linus Pauling, reference 1; Ralph W. Dornte, J. Am. Chem. Soc. **55**, 4126 (1933).

[6] L. Bewilogua, reference 3; also see Phys. Zeits. **32**, 740 (1931).

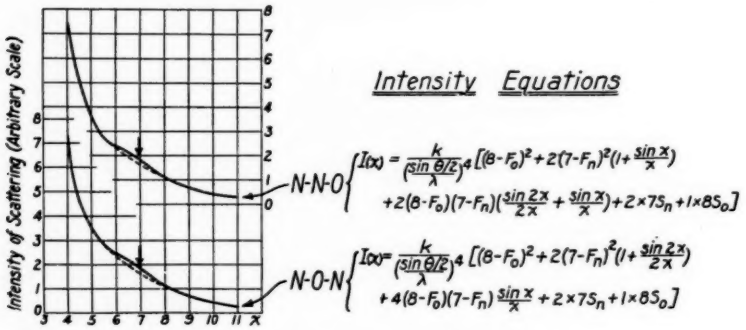

FIG. 1. Theoretical electron scattering curves for N_2O where $x=4\pi(1.1A)\ (\sin\theta/2)/\lambda$.

atomic length for incoherent scattering and is given by $b_i=0.176/Z_i^{\frac{1}{2}}$. $S(\nu_i)$ is a function of the parameter ν_i which has the value 0 for $\nu_i=0$ but converges to unity for large values of ν_i. k is a constant. The second term in the above equation expresses the amount of incoherent scattering.

The experimental apparatus used has already been described,[7] in which 20–35 kv cathode rays were projected through the beam of molecules under consideration. Scattering produced at small angles was recorded on a photographic plate located 26.2 cm from the scattering region and the diameter of the diffraction rings were measured by means of a recording microphotometer.

NITROUS OXIDE

Wierl[8] has obtained electron scattering from N_2O and found a diffraction ring occurring at $(1/\lambda)\sin\theta/2=0.468$ giving an N−N distance of 2.38 ± 0.06A for a model of the form N−O−N. This result has been confirmed in the present work in which case a value of $(1/\lambda)\sin\theta/2=0.465\pm0.01$ was obtained. Unfortunately it is very difficult to distinguish between the two possible linear forms of the molecule as illustrated in Fig. 1. The calculations are represented by the curves for the two cases and the formulas used are also shown. F_i, the atomic scattering factors were obtained from the calculated values of James and Brindley.[9] The two curves are practically indistinguishable and therefore make differentiation between the two forms very difficult. This is caused by the fact that the nitrogen and oxygen atoms scatter in nearly the same manner so that interchanging them does not alter materially the intensity curves. Likewise for the molecular models to be considered below, although reasonable allocations have been given to the nitrogen atoms, the electron diffraction methods cannot exclude the possibility of other arrangements for the nitrogen atoms with the same interatomic distances.

Additional information on the structure of N_2O has been determined from other sources as follows: *Band Spectra.* From an investigation of the infrared spectrum of N_2O Snow[10] concluded that the molecule is linear and has the symmetrical form N−O−N. Later Plyler and Barker[11] extended the range of wave-lengths to include a number of bands not previously obtained. From the properties of the spectrum they found that the model N−N−O agreed more precisely with the observation than either the N−O−N structure or the triangular model. Badger on calculating the moment of inertia from Plyler and Barker's data arrived at the value of 66.7×10^{-40} g cm² which has been used by Pauling[12] to give a structure resonating between the Lewis structures :N̈::N::Ö: and :N:::N:Ö: where the N−N and N−O distances are 1.10 and 1.22A, respectively, consistent with the electron diffraction results. (2) *Electric Moment.* There is some disagreement among various

[7] S. B. Hendricks, Louis R. Maxwell, V. M. Mosley and M. E. Jefferson, J. Chem. Phys. **1**, 549 (1933).

[8] R. Wierl, reference 1.

[9] R. W. James and G. W. Brindley, Phil. Mag. **12**, 81 (1931).

[10] C. P. Snow, Proc. Roy. Soc. **A128**, 294 (1930).

[11] E. K. Plyler and E. F. Barker, Phys. Rev. **38**, 1827 (1931).

[12] Linus Pauling, Proc. Nat. Acad. Sci. **18**, 293, 498 (1932).

workers on the value of the permanent electric moment of N_2O. Braunmühl[13] obtained a value of 0.25×10^{-18} while later Ghosh, Mahanti and Mukherjee[14] as well as Schwingel and Williams[15] concluded that the electric moment is zero. However, recently Watson, Rao and Ramaswamy[16] find that the moment is not zero but has the small value of 0.17×10^{-18}. On the basis of a finite electric moment the model N−N−O appears to be most probable.

Nitrogen Dioxide

In the case of scattering from NO_2 it was necessary to shift the equilibrium, $2NO_2 \rightleftarrows N_2O_4$ toward high concentrations of NO_2. This was accomplished by streaming the vapor through a heating bath at approximately 175°C and then to the diffraction apparatus where the walls and tip of the molecular jet were maintained at about 150°C. Under these conditions the scattering observed was produced by NO_2 and photographs were taken with voltages ranging from 27 to 36 kv. From thirteen exposures there were obtained no visible diffraction rings within the range of $(1/\lambda)\sin\theta/2$ from 0 to 0.6. Microphotometer records made on three typical plates also showed no evidence of rings.

Fig. 2 shows the results of the calculations made for the determination of the structure of this molecule. As in the previous case the incoherent scattering has been included. From the set of curves obtained it is seen that curves Nos. 4 and 9 show no maxima while No. 3 exhibits only a faint prominence. The experimental results are not sufficient to distinguish among these three curves so that the photographs are in agreement with any of the following forms:

$$N-O=1.15A, \quad \alpha=120°$$
$$N-O=1.15A, \quad \alpha=90°$$
$$N-O=1.30A, \quad \alpha=90°$$

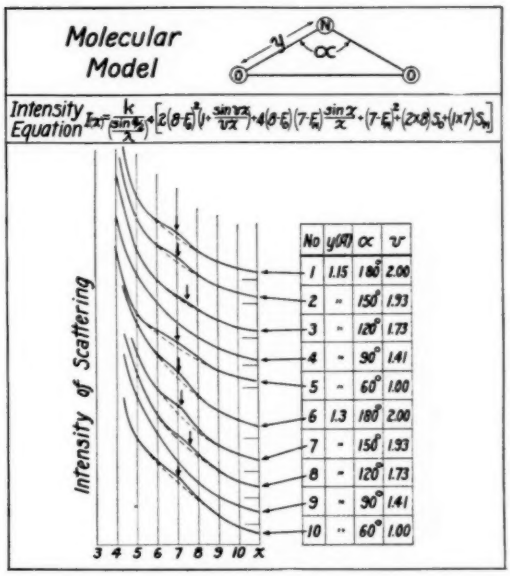

Fig. 2. Theoretical electron scattering curves for various models of NO_2 where $x=4\pi y(\sin\theta/2)/\lambda$.

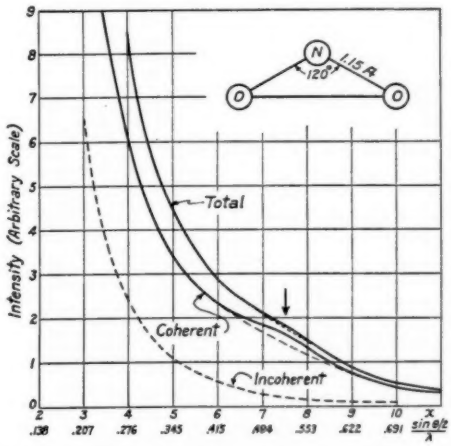

Fig. 3. Theoretical electron scattering curves for NO_2 illustrating an instance where the prominence of the diffraction ring is considerably decreased by the introduction of the incoherent scattering. Similar curves for benzene have been computed by Bewilogua.[3]

which are considered to be the most likely structures of the molecule.

An example of the effectiveness of the incoherent scattering in reducing the prominence of the diffraction ring as computed by only the coherent scattering is illustrated in Fig. 3. Thus the use of incoherent scattering causes the model $N-O=1.15A$, $\alpha=120°$ to come within the possible structures consistent with the experiments that otherwise would have been excluded.

[13] V. Braunmühl, Phys. Zeits. **28**, 141 (1927).

[14] P. N. Ghosh, P. C. Mahanti and B. C. Mukherjee, Zeits. f. Physik **58**, 200 (1929).

[15] C. H. Schwingel and J. W. Williams, Phys. Rev. **35**, 855 (1933).

[16] For a more complete discussion of the electric moment of N_2O see H. E. Watson, G. G. Rao and K. L. Ramaswamy, Proc. Roy. Soc. **A143**, 558 (1934).

TABLE I. *Comparison of various methods used for determining the theoretical position of electron diffraction rings.*

Molecule	Position of Diffraction Ring (x)			
NO_2	Coherent scattering[1]	Approximate solution[2]	Complete solution[3]	Error introduced by approx. sol.
$\alpha = 90°$, N−O=1.15A	6.0 (weak)	7.6	none	—
$\alpha = 120°$, N−O=1.15A	7.5	8.0	7.5 (very weak)	6.7%
$\alpha = 150°$, N−O=1.15A	7.1	7.5	7.1	5.6%
$\alpha = 90°$, N−O=1.30A	none	7.6	none	—
$\alpha = 120°$, N−O=1.30A	7.5	8.0	7.58	5.5%
$\alpha = 150°$, N−O=1.30A	7.1	7.5	7.2	4.2%

[1] ψ_i expressed completely.
[2] Coherent scattering with ψ_i replaced by Z_i, incoherent scattering omitted.
[3] Both coherent and incoherent scattering included with ψ_i expressed completely.

Table I shows a comparison of the different methods used for computing the diameter of the diffraction rings. The error introduced by the simplified treatment varies from 4 to 6 percent for the cases considered here and is not sufficiently exact to indicate those models which will produce no interference maxima. Considerable information is thereby lost by such treatment since the absence of diffraction rings may be equally important for structure determinations.

From a consideration of the values of the dielectric constant and index of refraction of NO_2 Ghosh and Mahanti[17] have predicted that the molecule is not linear and that the electric moment should be 0.62×10^{-18}, while recently Zahn[18] has found the electric moment to be 0.3×10^{-18} agreeing with a triangular model.

From studies of the infrared absorption spectra Bailey and Cassie[19] suggested that the molecule is linear with an N−O distance of 1.1A, a model which is definitely excluded by the electron diffraction results. Whereas Harris, Benedict and King[20] who examined the absorption bands of NO_2 under high resolution conclude that the molecule is not arranged in a linear form.

NITROGEN TETROXIDE

In order to obtain electron diffraction from N_2O_4 the heating bath and molecular jet were permitted to cool down to room temperature. The source of liquid N_2O_4 in the boiler was maintained at approximately its boiling point 21.5°C or atmospheric pressure, in which case there exists a mixture of 75 percent N_2O_4 and 25 percent NO_2. However, this pressure was reduced before the gas reached the molecular jet and was further reduced at the region in the diffraction chamber where the scattering occurred. Under these conditions a diffraction ring was obtained which is illustrated by the microphotometer record shown in Fig. 4.

Fourteen photographs were taken for wavelengths varying from 0.066A to 0.073A and the average value of $(1/\lambda)\sin\theta/2$ was found to be 0.455 ± 0.01. A complete set of calculated scattering curves are shown in Fig. 5, together with the position of the experimental diffraction ring for comparison. Since these computations were made for pure N_2O_4 a direct comparison is not justifiable until the amount and effect of NO_2 present is determined. The concentration of NO_2 can be obtained from an estimate of the pressure in the diffraction region. Lenard[21] has found a

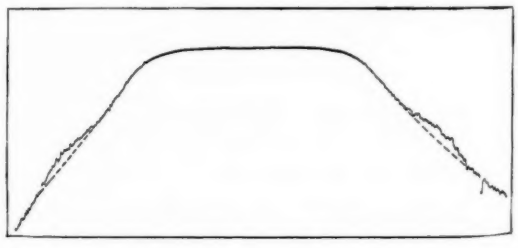

FIG. 4. Densitometer record for N_2O_4.

[17] P. N. Ghosh and P. C. Mahanti, Phys. Zeits. **30**, 531 (1929).
[18] C. T. Zahn, Phys. Zeits. **34**, 461 (1933).
[19] C. R. Bailey and A. B. D. Cassie, Nature **131**, 239 (1933).
[20] Louis Harris, W. S. Benedict and G. W. King, Nature **131**, 621 (1933).
[21] P. Lenard, Ann. d. Physik **12**, 714 (1903).

TABLE II. *Theoretical electron diffraction maxima from N_2O_4, NO_2 mixtures.*

Model No. of N_2O_4	Position of Maximum (x) 100% N_2O_4	50% N_2O_4, 50% NO_2	25% N_2O_4, 75% NO_2	10% N_2O_4, 90% NO_2
1	7.5	7.5	7.45	7.5
2	8.1	8.0	8.05	none
3	6.8	7.0	7.05	"
6	7.4	7.3	7.2	7.6 (weak)
7	6.4	6.45	none	none
8	7.0	7.0	6.9	"
9	6.5	6.8	7.0 (weak)	"
10	6.0	6.1	none	"

Experimental position 6.58±0.16; Model No. 3 used for NO_2.

value of 0.005 cm^{-1} per mm Hg for the specific absorption coefficient of air for 30 kv electrons. Assuming that air has approximately the same absorption as $N_2O_4 \rightleftarrows 2NO_2$, it is then possible to estimate the pressure of the diffraction region. The diameter of the opening in the molecular jet was 0.4 mm with the beam diverging in a manner approximating the cosine distribution law. The electron beam clears the opening of the jet by less than $\frac{1}{2}$ mm so that the depth of the beam at the point of scattering can be taken to be about 2 mm. If one further assumes that the primary beam intensity is decreased by 10 percent in order to yield a diffraction pattern then the pressure in the diffraction region using Lenard's data should be 0.14 atmosphere, in which case there would be not less than 50 percent dissociation in the region of diffraction. If the pressure were reduced to as low as 0.01 atmospheres the gas would be 90 percent dissociated. The effect on the position of the N_2O_4 diffraction ring by the addition of NO_2 is exemplified in Table II. The model chosen for NO_2 was the N−O=1.15A, $\alpha=120°$. Decreasing the percentage of N_2O_4 results chiefly in the reduction in size of the prominences rather than changing materially their positions. Even for the extreme case of 10 percent N_2O_4 many of the maxima have been entirely lost; however those which are still retained have not been appreciably displaced.

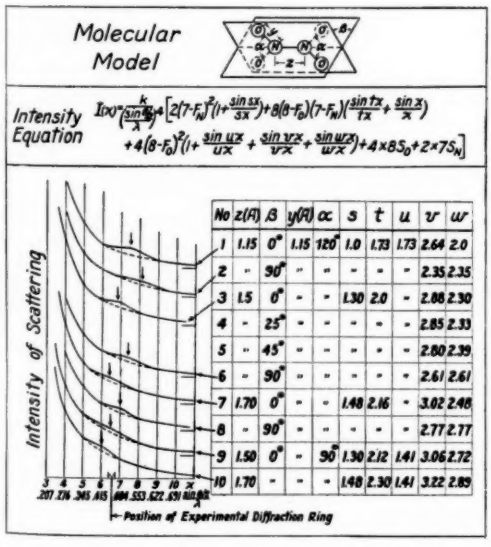

No	z(A)	β	y(A)	α	s	t	u	v	w
1	1.15	0°	1.15	120°	1.0	1.73	1.73	2.64	2.0
2	"	90°	"	"	"	"	"	2.35	2.35
3	1.5	0°	"	"	1.30	2.0	"	2.88	2.30
4	"	25°	"	"	"	"	"	2.85	2.33
5	"	45°	"	"	"	"	"	2.80	2.39
6	"	90°	"	"	"	"	"	2.61	2.61
7	1.70	0°	"	"	1.48	2.16	"	3.02	2.48
8	"	90°	"	"	"	"	"	2.77	2.77
9	1.50	0°	"	90°	1.30	2.12	1.41	3.06	2.72
10	1.70	"	"	"	1.48	2.30	1.41	3.22	2.85

FIG. 5. Theoretical electron scattering curves for various models of N_2O_4 where $x=4\pi y(\sin\theta/2)/\lambda$. A comparison with the position of the experimental diffraction maxima should be made after consulting Table II which shows the effect of the presence of NO_2.

From a consideration of these computations we arrive at the following possible structures of N_2O_4:

N−N=1.6A, $\beta=0°$ N−O=1.15A, $\alpha=120°$
N−N=1.7A, $45°<\beta<90°$, N−O=1.15A, $\alpha=120°$
N−N=1.6A, $\beta=0°$ N−O=1.15A, $\alpha=90°$.

This is equivalent to specifying that the N−N distance is 1.6 to 1.7A without definitely fixing the angular relationship between the two NO_2 groups.

Sutherland[22] has measured the infrared absorption spectrum and Raman scattering of N_2O_4 and found that the molecular form O_2N-NO_2 was definitely more probable than the other radically different structures such as O−N−O−NO_2 and O−N−O−O−N−O. The first form is preferred on account of the ease of dissociation into NO_2 and satisfactorily explains the outstanding features of the infrared and Raman

[22] G. B. B. M. Sutherland, Proc. Roy. Soc. **A141**, 342, 535 (1933).

scattering. Also evidence was obtained against location of the NO_2 groups at right angles to each other, i.e., $\beta = 90°$. Harris and King[23] have recently concluded from the infrared absorption spectra that the NO_2 groups may not lie in the same plane and that they are joined together by the nitrogen atoms.

From x-ray diffraction photographs of solid N_2O_4 Vegard[24] has proposed that the crystal lattice is built up of linear and symmetrical NO_2 groups. Hendricks[25] has interpreted Vegard's results as signifying that the solid is made of O_2N-NO_2 groups with $\alpha = 120°$, β from 0 to 25° and the N−N distance within the range of 1.1 to 1.7A.

Nitrogen Pentoxide

N_2O_5[26] gave an interference pattern quite similar to N_2O_4, with a single diffraction ring occurring at a slightly greater angle, giving $(1/\lambda)\sin\theta/2 = 0.474 \pm 0.004$. The temperature of the substance was raised to between 25° and 40°C which afforded sufficient vapor pressure to obtain diffraction. However, the substance was maintained at these temperatures for less than 10 minutes which was time enough to obtain a set of photographs. This prevented the formation of any undesirable amount of products of decomposition. Fig. 6 shows a typical densitometer record of N_2O_5 while the theoretical scattering curves are given in Fig. 7. Molecular models Nos. 2 and 8 give the best agreement with the experiment although the position of the experimental maxima is definitely smaller than the theoretical value expressed in terms of the variable $x = 4\pi y(\sin\theta/2)/\lambda$. y was taken to be 1.15A, one of the possible distances for the NO_2 group as previously determined. If we now substitute in this equation $x = 7$ (theoretical value), and $(\sin\theta/2)/\lambda = 0.474$ (experimental value) we obtain $y = 1.18$A. Since this distance is only slightly different from the assumed value, the position of the diffraction ring would not be appreciably altered by this change in the N−O distance of the NO_2 group. Thus we can arrive at a model in good agreement with the experimental result, namely N−O = 1.3 to 1.4A with $y = 1.18$A.

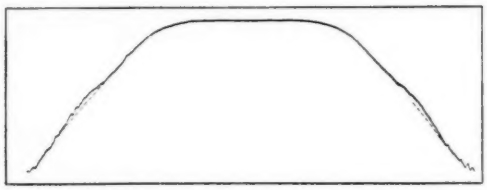

Fig. 6. Densitometer record for N_2O_5.

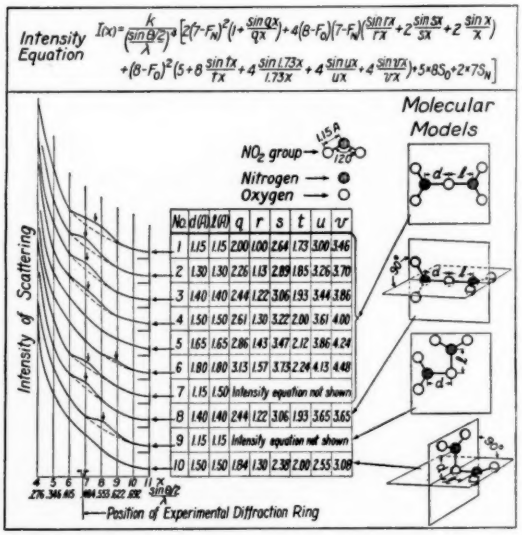

Fig. 7. Theoretical electron scattering curves for various models of N_2O_5 where $x = 4\pi(1.15\text{A})(\sin\theta/2)/\lambda$.

[23] Louis Harris and G. W. King, J. Chem. Phys. **2**, 51 (1934).

[24] L. Vegard, Zeits. f. Physik **68**, 184 (1931); **71**, 299 (1931).

[25] Sterling B. Hendricks, Zeits. f. Physik **70**,699 (1931).

[26] N_2O_5 was prepared by treating $N_2O_4 \leftrightarrows 2NO_2$ with ozone, after the method of Demetric Helbig, R. Accad. dei Lincei, Atti Scienze, (5a) **S12**, 211 (1903).

The Natural Separation of the Isotopes of Hydrogen. I. The Concentration of Deuterium in Benzene, Kerosene and Honey

MALCOLM DOLE, *Department of Chemistry, Northwestern University*
(Received March 29, 1934)

Waters obtained in the combustion of benzene, kerosene and honey have been analyzed for their deuterium content by density measurements. In all cases the concentration of deuterium is greater in these substances than it is in distilled water from Lake Michigan.

THE interesting discoveries of Lewis[1] and of Taylor, Swingle, Eyring and Frost[2] of the inability of living organisms to live or to grow in nearly pure deuterium oxide suggested the possibility of a natural selection of protium in preference to deuterium in the animal and vegetable kingdoms. In order to ascertain if any separation of the isotopes of hydrogen takes place in the organic world I began last December to analyze naturally occurring substances for their deuterium content. Meanwhile Washburn and Smith[3] in an investigation begun in August, 1932, were examining the sap and the dry wood of a willow tree for their deuterium content. A preliminary notice of this investigation states that water obtained from the sap is 2.8 parts per million heavier than ordinary water while water obtained from the combustion of the dry wood was 5.4 parts per million heavier than ordinary water. They also proved that this increase of density was due to an increase in percentage of deuterium in the water.

I have examined honey, kerosene and benzene and find, similarly to Washburn and Smith, that water obtained from the combustion of these substances is in all cases *heavier* than ordinary water. These results were not expected on the basis of the physiological experiments carried out in pure deuterium oxide since if the deuterium had been rejected instead of utilized in the synthesis of cellulose, honey, benzene and kerosene the water resulting from the combustion of these substances would have been *lighter* than ordinary water. However, experiments[4] of Barnes, of Meyer and of Richards on the physiological behavior of *Spirogyra sp.*, *Aspergillus sp.* and *Saccharomyces cerevisiae* indicate that dilute solutions of deuterium oxide have a decided effect in accelerating or modifying the growth and development of these substances. If this is the case, one might expect that deuterium would be selected preferentially, thereby increasing the atomic weight of hydrogen in organic compounds and causing the density of water obtained by combustion to be greater than that of ordinary water. In this way it is possible to explain qualitatively the increase in the atomic weight of hydrogen reported by Washburn and Smith and by this paper.

EXPERIMENTAL

(a) Honey

Honey of an unknown origin was dropped at the rate of one drop every twenty seconds onto dull red hot copper oxide in a Pyrex tube through which a stream of dried tank oxygen was passed. The details of this burner are shown in Fig. 1 where *A* is the reservoir for the liquid honey, *B* is the tip from which the honey dropped onto the copper oxide *D*, *E* is a side tube to allow the tip *B* to be freed of tar or carbon by a blast of air, and *C* and *D* are inlets for oxygen. The copper oxide was electrically heated and the combustion

[1] G. N. Lewis, J. Am. Chem. Soc. **55**, 3503 (1933).
[2] H. S. Taylor, W. W. Swingle, Henry Eyring and A. A. Frost, J. Chem. Phys. **1**, 751 (1933).
[3] E. W. Washburn and E. R. Smith, Science **79**, 2043 (1934).
[4] T. C. Barnes, J. Am. Chem. Soc. **55**, 4332 (1933); Am. J. Bot. **20**, 681 (1933); S. L. Meyer, Science **79**, 210 (1934); O. W. Richards, Am. J. Bot. **20**, 679 (1933).

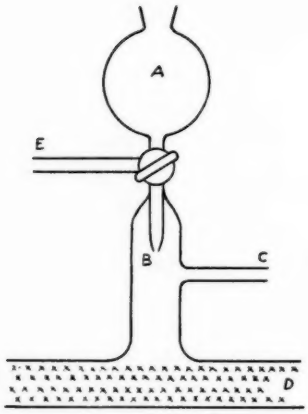

FIG. 1. Burner for honey.

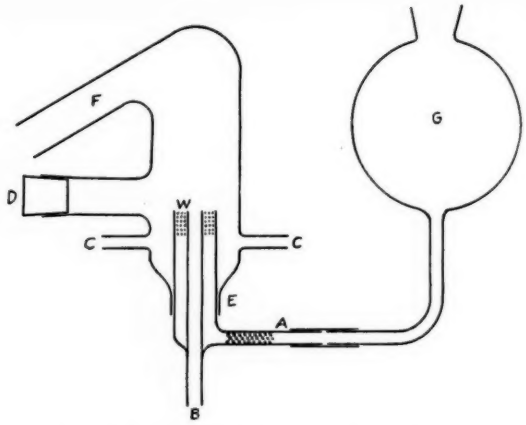

FIG. 2. Burner for kerosene and benzene.

was allowed to run continuously for seventy-two hours until 570 cc of water had been condensed. The formation of tar and carbon at *B* or on the inside walls of the upright tube was prevented by passing oxygen in at *C* in addition to at *D* and by keeping the copper oxide hot enough so that the honey burst into a little flame as each drop fell on the copper oxide. The condensed water contained appreciable quantities of organic matter judging from its color and odor. It was first distilled in such a way that the vapors were mixed with dried oxygen and then passed through a 55 cm column of dull red hot copper oxide. From this point on the purification consisted of ten distillations from alkaline potassium permanganate, a distillation in vacuum followed by distillations from alkaline potassium permanganate and a dilute solution of phosphoric acid. No change in density could be detected between the distillation in vacuum and the subsequent distillation from phosphoric acid.

(b) Kerosene

Kerosene from the Oklahoma oil fields was burnt at the surface of a sintered glass wick in an apparatus, the details of which are shown in Fig. 2 where *A* is the inlet for kerosene, *B* and *C* are air inlets, *W* is the sintered glass wick made of ground Pyrex glass and *A* represents a packing of string to prevent a too rapid flow of kerosene into the burner. The burner was inserted into the combustion apparatus and held in place by a rubber connection at *E*. Air was admitted into the apparatus at *B* and *C*, the speed of flow through *B* could be controlled independently. The cork stopper at *D* could be removed to light the flame. The vapors were led to an efficient condenser by means of the tube *F*. It was impossible to obtain a satisfactory combustion of kerosene in an atmosphere of pure oxygen due to the deposition of carbon in tree-like growths on the surface of the wick. The level of the kerosene in the reservoir, *G* was maintained at a height three inches above the top of the wick in order to provide the necessary pressure to force the kerosene up onto the sintered glass wick. About 600 cc of kerosene were burnt over a period of 72 hours and about 500 cc of water were obtained. The water was purified in the same way that the honey water was purified except that no distillation in vacuum was carried out and only seven redistillations were considered necessary.

(c) Benzene

Mallinckrodt thiophene free benzene obtained as a by-product in the distillation of coal was burnt in the apparatus illustrated in Fig. 2. Due to the relatively high percent of carbon in benzene the combustion was more difficult, required more air and gave rise to considerably more soot than did the combustion of kerosene. In order to prevent the large amount of uncondensable gases such as carbon dioxide and nitrogen from carrying off too much of the desired water vapor, the gases were not passed through the water collecting flask but were by-passed over it. The water was first filtered to remove as

much carbon as possible, then distilled twice from alkaline permanganate and its density measured. Two more redistillations from alkaline permanganate did not measurably alter the density.

(d) Tests of the purity of the water

Since the measurement of the relative density of water may be carried out with an error of less than a part per million (*vide infra*), the only uncertainty in the results reported in this paper is the question of the purity of the water. The density of the benzene water after the second and fourth distillations was 7.9 parts per million heavier than ordinary water. In order to see if this difference in density was caused by impurities, about 250 cc of this benzene water were electrolyzed at a current of nine amperes between a lead anode and a nickel cathode. The mixed hydrogen and oxygen gases were next washed in three tall towers containing, respectively, distilled water, ten percent potassium hydroxide solution and concentrated sulfuric acid. Finally the gases were converted back to water over a copper catalyst. The density of this water after a distillation from alkaline permanganate was still greater than that of ordinary water treated in the same way to the extent of 3.6 parts per million. Thus, 250 cc of ordinary water electrolyzed until 3.5 cc remained in the electrolysis cell decreased in density 7.7 parts per million while the benzene water electrolyzed until 4.0 cc remained in the electrolysis cell decreased in density 12.0 parts per million. It is difficult to decide how much of this decrease is due to a separation of isotopes and how much to elimination of impurities.[5] The point of interest is that the benzene water was still heavier than ordinary water similarly treated.

Another method of testing the effectiveness of the methods outlined above for purifying water is to contaminate some ordinary water deliberately and then to study the rapidity with which it can be made pure again. To 500 cc of ordinary distilled water about 1 cc of the following chemicals was added, acetic acid, ethyl alcohol, benzoic acid, formaldehyde, acetaldehyde, benzene, ammonium nitrate, sodium nitrate and sodium nitrite. To the solution enough potassium permanganate was added to give a permanent purple color and a considerable quantity of barium hydroxide was added. Distillation from this mixture was difficult due to the presence of a large amount of manganese dioxide. After a second distillation from alkaline permanganate, the water was four parts per million heavier than pure water, after a third distillation the difference in density was only one part per million while after a fourth distillation from alkaline permanganate the density of the previously contaminated water was equal to that of pure water within the experimental uncertainty. Apparently four redistillations from alkaline permanganate are sufficient to free water from considerable amounts of impurities.

(e) Density measurements

The density was measured by the totally immersed float method; the density of the water being adjusted to that of the float by altering the temperature of the water according to the method first used by Richards and Shipley.[6] A 14 cc Pyrex float weighted with mercury was used. The float was aged by heating at 110° in an electric oven for twenty-four hours and was steamed out before use. No appreciable change in the temperature at which the float and water had the same density could be detected over a period of three months, nor could any definite relation between the barometric pressure and the equilibrium temperature be discovered. (See Table I.) Any possible errors due to a change in the barometric pressure or to a change in the density of the float were eliminated by always

[5] The difference between a decrease in density of 7.7 and 12.0 parts per million seems large. However, if the decrease in density is due entirely to a separation of the isotopes of hydrogen, and if ordinary water is 20 parts per million and benzene water 27.9 parts per million heavier than pure protium oxide then a decrease of 7.7 parts in 20 parts is a decrease of 39 percent while a decrease of 12.0 parts in 27.9 parts is a decrease of 43 percent. From this standpoint the greater decrease in density of the benzene water on electrolysis does not indicate that the benzene water was more impure than the ordinary water, but merely that it contained more deuterium. In other words the benzene water and ordinary water lost nearly the same percentage of their deuterium content on electrolysis.

[6] T. W. Richards and J. W. Shipley, J. Am. Chem. Soc. **34**, 599 (1912).

TABLE I. *Buoyancy float data for ordinary water.*

Exp. No.	Date	Barometer	No. of redistillations	Temperature 2.700° Beckmann =23.412°C
1	1/5	742	one	2.705
2	1/12	742	one	2.703
3	1/13	736	one	2.735 (?)
4	1/15	751	one	2.693
5	1/17	757	one	2.695
6	1/19	751	one	2.697
7	1/26	746	eight	2.697
8	2/8	759	one	2.694
9	2/8	759	two	2.697
10	2/14	742	three	2.703
11	2/17	752	four	2.700
12	2/17	752	five	2.736 (?)
13	2/19	753	six	2.693
14	2/19	753	seven	2.697
15	3/7	752	one	2.704
16	3/9	755	one	2.702
17	3/14	759	one	2.702
18	3/17	738	one	2.713
19	3/21	742	one	2.714

redetermining the equilibrium temperature for pure water immediately before making a density measurement of the various waters under investigation. The float cylinder was surrounded by two water baths according to the method of Lamb and Lee.[7] In agreement with them it was found necessary to eliminate all vibrations by stopping the stirring motor before observing the motion of the float. During the observation period no temperature control was possible, but tests proved that the temperature of the water in the float cylinder changed only 0.002° in twenty minutes under unusually adverse conditions. The time necessary for the observation of the float was five to ten minutes. After immersing the float in the water, the cylinder was exhausted (at room temperature) until the water boiled vigorously. The float was never allowed to come to the surface of the water after this boiling out, because it was found that tiny air bubbles might adhere to the top of the float when the float was pushed below the surface of the water.

The reproducibility of the measurements for laboratory distilled water are indicated in Table I where the first column gives the number of the experiment, column two the date, column three the barometric pressure, column four the number of redistillations of the laboratory distilled water previous to the measurement, and column five the equilibrium temperatures as read on the Beckmann thermometer. In an actual measurement the temperature was changed in increments of 0.005° and the equilibrium temperature was estimated to 0.001°. The high data for experiments 3 and 12 may be due to small air bubbles adhering to the top of the float. It was after the twelfth experiment that the float was always kept totally immersed. Variations greater than 0.005° are probably due to changes in the barometric pressure. The increase in the temperature between experiments 14 and 15 may be due to a slight change in the density of the float.

The values for the rise in temperature necessary to bring the density of the water obtained in the combustion of honey, kerosene and benzene to the density of ordinary water are given in Table II. For purposes of comparison data obtained with water deliberately contaminated as related above are also given.

TABLE II. *Buoyancy float data for various types of water.*

Exp. No.	Date	Redistillations	$\Delta t°$
Water from Kerosene			
1	2/14	3	0.030
2	2/17	4	.028
3	2/17	5	.027
4	2/19	6	.025
5	2/19	7	.025
Accepted value = 0.025			
Density increment = 6.2 parts per million			
Water from Benzene			
1	3/7	2	0.031
2	3/9	4	.031
Accepted value = 0.031			
Density increment = 7.9 parts per million			

Exp. No.	Date	Redistillations	$\Delta t°$
Water from Honey			
1	1/13	3	0.055
2	1/15	5	.044
3	1/19	8	.023
4	1/20	9	.024
5	1/26	10	.028
6	2/8	12	.016
7	2/19	14	.018
Accepted value = 0.017			
Density increment = 4.1 parts per million			
Contaminated ordinary water			
1	3/16	1	0.14
2	3/16	2	.019
3	3/17	3	.006
4	3/21	4	−.003

CONCLUSIONS

The data indicate a definite increase in the atomic weight of hydrogen due to a natural isotopic separation. Bleakney and Gould[8] estimate the concentration of deuterium in rain water to be one part in five thousand parts of hydrogen. If the water of Lake Michigan con-

[7] A. B. Lamb and R. E. Lee, J. Am. Chem. Soc. **35**, 1666 (1913).

[8] W. Bleakney and A. J. Gould, Phys. Rev. **44**, 265 (1933).

tains this concentration of deuterium, it is possible to calculate the concentration of deuterium in kerosene, benzene and honey by means of the equation

$$\Delta s = 0.1056x \qquad (1)$$

given by Lewis and Luten.[9] In Eq. (1) Δs is the density increment between the water under consideration and pure protium oxide, and x is the mole fraction of deuterium oxide or the atom fraction of deuterium. Calculations for kerosene water yield for Δs 26 parts per million and for x 1.3 parts in 5000. Thus there is roughly 30 percent more deuterium in Oklahoma kerosene than there is in ordinary water. Similar calculations yield for the concentration of deuterium in benzene 1.4 and in honey 1.2 parts of deuterium per 5000 parts of hydrogen. In the case of water from honey we are assuming that the increase in density is due entirely to an increase in the concentration of deuterium. The work of Washburn and Smith indicates that this assumption is probably correct.

Further experiments are planned. It is hoped that the results of this paper and additional results will shed light on the origin of petroleum.

[9] G. N. Lewis and D. B. Luten, Jr., J. Am. Chem. Soc. **55**, 5062 (1933).

Continuous Flow Methods of Concentrating Deuterium

LEIGH C. ANDERSON, J. O. HALFORD AND JOHN R. BATES, *Department of Chemistry, University of Michigan*

(Received March 2, 1934)

Experimental arrangements for the concentration of deuterium by electrolysis in a continuous flow system are described. These are found to be as efficient as straight electrolysis in single cells and involve considerably less manual labor. An arrangement for the recovery of off hydrogen of high deuterium content which is practically free from danger of explosion is also given.

SINCE Washburn and Urey discovered that the deuterium content[1] of an aqueous solution could be increased by electrolysis, due to the preferential liberation of protium at the cathode, several investigators have described apparatus for carrying out this concentration. The first stages which involve relatively large volumes of solution are the most cumbersome. Two types of apparatus have been developed in this laboratory which allow the concentration to be performed in a continuous and practically automatic manner. Neither type requires a low voltage source of direct current capable of delivering hundreds of amperes, a source which is not readily available in many laboratories, and which is required when one employs the apparatus described by Lewis and MacDonald[2] or that of Harkins and Doede.[3] The procedure used by Taylor, Eyring and Frost,[4] eliminates the need of such an electrical supply but introduces a considerable amount of labor in handling a large number of cells and, furthermore, the cooling tanks quickly become objectionable when the water supply is extremely hard.

The first of the two types of unit which we have developed is composed of cells illustrated in Fig. 1. The cathode *B* is an 18-inch length of ordinary 1-inch water pipe designated in the trade as wrought iron, but in reality a low carbon steel. (So-called pure wrought iron pipe was substituted with little or no benefit.) This is surrounded by a glass condenser jacket *A* for cooling. The bottom of the pipe is fitted with a rubber stopper through which pass two 7 mm glass tubes. The centered tube *C* acts both as a support for the anode and as the inlet tube for the alkaline electrolyte; the other tube is the outlet. The anode *D* is formed from two 3-foot lengths of 18 gauge nickel wire which extend through the rubber stopper and are wound around the center tube and two strips of nickel ribbon. These latter

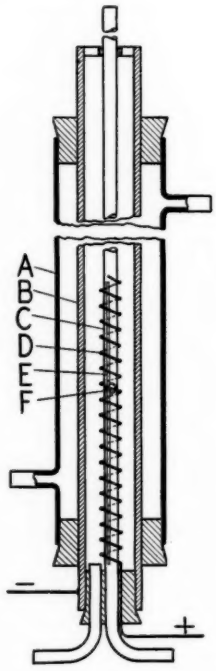

FIG. 1.

[1] Washburn and Urey, Proc. Nat. Acad. Sci. **18**, 496 (1932).
[2] Lewis and MacDonald, J. Chem. Phys. **1**, 341 (1933).
[3] Harkins and Doede, J. Am. Chem. Soc. **55**, 4330 (1933).
[4] Taylor, Eyring and Frost, J. Chem. Phys. **1**, 823 (1933).

serve to equalize the potential along the whole electrode.

For convenience in handling, a bank of ten such cells is mounted in series as regards flow of electricity, alkali and cooling water. The alkali flowing in the center tube and emerging from the orifice F is partially electrolyzed in each cell before flowing out and into the next cell. Because of the height of the inlet orifice and the stirring due to the gas evolution, no channeling between inlet and outlet may be expected. The rates of inflow and outflow through the entire bank are adjusted to the rate of electrical input so that any desired concentration of alkali may be reached at the end of the bank. The inflow is regulated by means of an 8-liter Mariotte bottle, which keeps a constant head at the inlet and into which alkali is fed at a rate equal to or less than that of consumption. This removes any possibility of overflow in the cells due to small alterations in current, etc.

The factor limiting the amount of current which may be put through such a bank of cells is the back pressure which is built up in the alkali line and which may amount to a head of several inches. This is probably due to mechanical difficulties involved in the evolution of the electrolytic gas. In practice, we find that a current of about twenty amperes gives a very satisfactory performance. This current is obtained when a potential of 220 volts is applied to three banks of twenty cells each, with a two percent alkali solution being fed to, and a sixteen percent alkali solution being withdrawn from each of the banks.

The second type of unit that we have developed consists of a box four inches wide, six inches deep and twenty-five inches long made of hard rubber and with the sides slotted on the inside at intervals of one-half inch to hold nickel sheet electrodes. Cooling is accomplished internally by means of five 10 mm glass tubes running lengthwise through the box and through holes in each electrode. The electrodes are made up in two identical halves to permit easy assembly of the cooling tubes. A dilute alkali solution is fed into one end continuously and flows from one cell to the next through a narrow space left around each of the cooling tubes. A concentration gradient is built up along the box and the concentrated material is removed from the other end at any desired alkali concentration (and, of course, increased deuterium content) below that of saturation of the electrolyte. Such a unit will carry five amperes without overheating, and this current is obtained with a potential of 110 volts across the box.

The theoretical efficiency of any continuous method of electrolytic fractionation of the hydrogen isotopes is bound to be lower than that of straight electrolytic concentration in a single cell. This is due to the fact that a more dilute solution of the heavier isotope is being fed constantly to a more concentrated mixture. In the limiting case, it is obvious that when the entering liquid has a deuterium content equal to the gases evolved no further concentration occurs. However, in the "pipe" method described this latter condition is by no means approached and our actual efficiency seems to be as good or better than electrolysis in open single cells, due to less loss from spraying of the electrolyte and less evaporation because of more efficient cooling. Best results are obtained, of course, when the volume ratio of input to output in a given unit is small, but even with this ratio at seven for a bank of twenty cells, we find the concentration ratio of deuterium is about five, an extremely satisfactory factor.

Of the two types of unit the first is undoubtedly to be preferred. The chief difficulty encountered with it is the regulation of the outflow. Since, with a current of 20 amperes the outflow from a bank of twenty cells is only 700 cc of sixteen percent alkali a day, the regulation must be made of a rather small rate, about a drop every ten seconds, and this must be kept constant, as the concentration ratio is dependent almost solely upon it. The chief advantage of the box unit is that the regulation of outflow need not be accurate since this can be adjusted by removal of larger amounts at a single time when inspection shows this to be necessary. Its disadvantage lies in lack of adequate cooling and consequent limitation of the current to about five or six amperes. The pipe unit has still another consideration to recommend it. It may be used at higher concentrations of deuterium when it is necessary to recover the gases produced. This may be effected by recombining the mixed

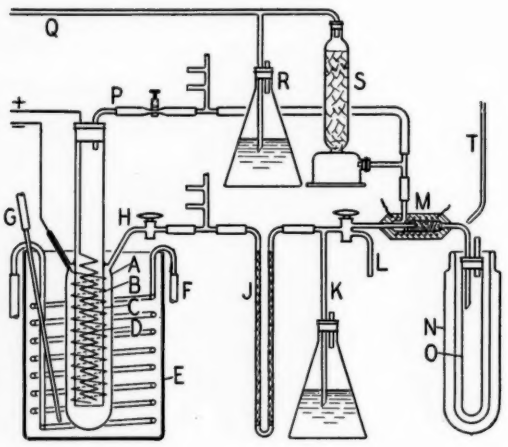

FIG. 2.

hydrogen and oxygen as described by Taylor, Eyring and Frost,[4] and by Eyring and Topley.[5] However, we have not used their procedure in this laboratory, preferring the increased safety factor introduced by separating the hydrogen and oxygen and burning the hydrogen from a quartz jet in the presence of air or oxygen. At still higher concentrations where there is insufficient gas evolution to make a flame, we have used the method illustrated in Fig. 2, using platinized asbestos as a catalyst for burning the hydrogen.

The cathode *B* consists of iron wire wound around the glass tube *C* which is sealed inside the cell *A*; the anode *D* is either a spiral of nickel wire or a platinum gauze cylinder which is inserted inside the glass partition. When wire spirals are used, the top and bottom wires are joined together in order that the potential may be more uniform throughout the electrode. *J*, *K* and *L* are, respectively, a spray trap, a safety flask and an outlet for flushing out the hydrogen line at the start of operation. The oxygen passes through the tube marked *P*. The hydrogen and oxygen combine in the catalytic chamber *M* at the end of the capillary platinum tube from which the hydrogen emerges. A stream of air is directed through *T* to cool the vapors partially. The receiver *O* is kept in an ice-filled vacuum bottle *N*. A small excess of oxygen is introduced (through *Q*, *R* and *S*) to insure complete combustion of the hydrogen. Although the electrolytic cells necessary for the separation of the gases introduce more electrical resistance than those in which the gases come off together, this difficulty has not been at all troublesome and a current of eight or nine amperes gives no undue heating of the cells. Several of these cells are mounted in series electrically, the hydrogen as well as the oxygen from all cells being fed to the same combiner, whether flame or catalytic. With the smaller quantities of material that are available at the higher concentrations of deuterium, we have not adopted a flow method although this process could be introduced here also.

[5] Eyring and Topley, J. Am. Chem. Soc. **55**, 5058 (1933).

The Homogeneous Unimolecular Decomposition of Gaseous Alkyl Nitrites. II. The Decomposition of Ethyl Nitrite

E. W. R. Steacie and G. T. Shaw, *Physical Chemistry Laboratory, McGill University, Montreal*

(Received April 10, 1934)

The thermal decomposition of gaseous ethyl nitrite is a homogeneous first order reaction. It proceeds at a conveniently measurable rate between 190 and 240°C. The overall reaction is mainly

$$C_2H_5NO_2 = NO + \tfrac{1}{2}CH_3CHO + \tfrac{1}{2}C_2H_5OH.$$

The rate of reaction is given by

$$k = 1.39 \times 10^{14} e^{-37{,}700/RT} \text{ sec.}^{-1}$$

There is no falling off in rate down to 5 cm pressure. On account of their similarity and simplicity the comparison of the decompositions of methyl and ethyl nitrite is of considerable interest. Further work is in progress on the propyl and butyl nitrites.

Introduction

It is of considerable interest to investigate the homogeneous unimolecular decomposition of a series of related chemical compounds. The only series so far investigated is that of the aliphatic ethers.[1] The ether decompositions, however, are complicated, and in consequence it is difficult to make comparisons between them. It has recently been shown[2] that the decomposition of methyl nitrite is a homogeneous first order reaction. The decomposition is simple, the rate determining step being apparently the splitting off of nitric oxide, and hence it is of interest to investigate the decomposition of other alkyl nitrites. The present paper deals with ethyl nitrite.

Experimental

Reaction velocities were measured as before by observing the rate of pressure change in a system at constant volume. The reaction vessels were Pyrex bulbs having a capacity of about 125 cc. The apparatus was similar to that used in a number of previous investigations.[3] The required temperatures were obtained by the use of a well stirred oil bath, heated electrically. Temperatures were measured with standard mercury thermometers. The temperature could be maintained constant to within 0.25°C.

Ethyl nitrite was prepared by the addition of a solution of nitrous acid to ethyl alcohol. The gas evolved was purified by passing it through a 50 percent sodium hydroxide solution, followed by a 40 percent ferrous sulphate solution to remove nitrogen oxides. It was then roughly dried by passage over calcium chloride. The gas was then condensed and fractionally distilled twice. During the course of the investigation the ethyl nitrite was stored as a liquid in a cooled bulb.

Experimental Results

The products of the reaction

Since the form of the reaction rate curves and the total pressure increase at completion did not vary with temperature or pressure, as will be shown later, it follows that there cannot be much variation in the products of reaction with varying conditions.

[1] Hinshelwood and co-workers, Proc. Roy. Soc. **A114**, 84 (1927), **A115**, 215 (1927), J. Chem. Soc. **1929**, 1804. Steacie, J. Phys. Chem. **36**, 1562 (1932), J. Chem. Phys. **1**, 313, 618 (1933). Kassel, J. A. C. S. **54**, 3641 (1932). Ure, J. Phys. Chem. **37**, 1169, 1183 (1933).

[2] Steacie and Shaw, Proc. Roy. Soc. (London), in press.

[3] Steacie, Can. J. Research **6**, 265 (1932).

Some typical analyses of the gaseous products at completion follow:

NO, %	94.2	88.0
CO, %	1.3	3.3
Residue, %	4.5	8.7

In the above analyses NO was determined by absorption with slightly acidified ferrous sulphate. Gas analysis in the presence of nitrogen oxides is necessarily difficult, and in view of this fact the above results are in satisfactory agreement. The gaseous products are very similar to those of the methyl nitrite decomposition, the average values for methyl nitrite being NO = 84 percent, CO = 7 percent, residue = 9 percent.

The condensable products of the reaction were determined by means of experiments in a special reaction vessel, so constructed that it could be washed out with water after each run. The washings gave a pronounced Schiff test for aldehydes. If the solution were warmed up to distill off aldehydes, and sulphuric acid added, a positive Schiff test was again obtained, pointing to the presence of alcohols which had been oxidized to aldehydes. By analogy with the methyl nitrite decomposition it may therefore be concluded that the condensable products consist of acetaldehyde and ethyl alcohol. This is supported by the fact that the condensable products were liquids, that ethyl alcohol could be detected by its odor, and that there was no sign of a deposit of paraformaldehyde.

We may therefore conclude that the reaction proceeds in a manner similar to that of methyl nitrite, *viz.*,

$$C_2H_5NO_2 = NO + \tfrac{1}{2}C_2H_5OH + \tfrac{1}{2}CH_3CHO.$$

This mechanism was confirmed by a determination of the relative amounts of liquid and gaseous products. A run was made at 235°C with an initial pressure of 27.0 cm. At completion the pressure was 51.5 cm, an increase of 24.5 cm. The reaction vessel was then cooled to −80°C. At this temperature the pressure was 9.98 cm. Calculating the pressure which this amount of gas would exert at 235°C, we obtain 26.3 cm. This is almost exactly equal to the initial pressure of ethyl nitrite. Hence, in agreement with the above mechanism, we obtain 1 molecule of non-condensable material from each molecule of ethyl nitrite. The reaction vessel was then heated to 13°C, and the pressure was found to be 23.6 cm. The calculated NO pressure at 13°C is 14.8 cm. At 13°C the vapor pressure of ethyl alcohol is 2.4 cm. Acetaldehyde should all be in the gas phase at this temperature. If we assume all the gas other than NO and alcohol vapor to be acetaldehyde, then the partial pressure of acetaldehyde at 13°C is 6.4 cm. This is somewhat less than half the NO as required by the above mechanism. However, considering the small amount of alcohol present, it is doubtful if vapor pressure equilibrium would really be reached, and hence the amount of acetaldehyde present is probably larger than that calculated. Finally, it was shown that all the products were gaseous at 87°C, as would be the case if ethyl alcohol were the remaining product.

It may therefore be concluded that the overall reaction is the one given previously. The mechanism is presumably the following:

$$C_2H_5NO_2 = C_2H_5O + NO \quad (1)$$

$$C_2H_5O = CH_3CHO + H \quad (2)$$

$$H + C_2H_5O = C_2H_5OH. \quad (3)$$

This is consistent with the work of Rice[4] and his collaborators on free radicals in the decomposition of organic compounds.

The pressure change accompanying the reaction

The mechanism given above would lead to a pressure increase of 100 percent at completion. Actually the observed pressure increases average about 86 percent. Some typical values are given in Table I.

TABLE I. *Maximum pressure increases.*

Temperature (°C)	Initial pressure (cm)	Maximum pressure increase (percent)
199.9	23.89	88.7
209.8	13.48	90.3
209.8	18.48	83.3
219.9	28.40	90.7
219.9	33.36	83.3
230.2	22.85	84.2
230.2	23.21	85.3
240.7	27.96	80.7
	Mean	85.8

[4] Rice *et al.*, J. A. C. S. **53**, 1959 (1931); **55**, 3035 (1933); **56**, 284 (1934).

If we assume that 86 percent pressure increase corresponds to complete reaction, then T_{25} and T_{50} (the times for the pressure to increase 25 and 50 percent, respectively) correspond to 29.1 and 58.2 percent reaction. Theoretically therefore T_{50}/T_{25} should be equal to 2.54 if the reaction is first order. Actually the mean ratio for all runs is 2.57. It therefore seems to be justifiable to use the values of T_{25} and T_{50} as a measure of the rate of reaction, and to assume that they correspond to 29.1 and 58.2 percent reaction, respectively.

The rate of reaction

Complete data for some typical runs are given in Table II. It will be seen that good first order constants are obtained. The summarized data for all runs are given in Table III.

The effect of pressure on the rate

The constancy of the values of the fractional times with varying pressure shows that the reaction is of the first order. If there is any falling off in rate at low pressures, it is of the order of magnitude of the experimental error. The reaction is under investigation at low pressures, and the results will be reported later.

TABLE II. *Data for typical runs.*

	Temperature = 209.8°C Initial pressure = 36.57 cm			Temperature = 219.9°C Initial pressure = 20.62 cm		
Time (min.)	ΔP (cm)	% reaction	k	ΔP (cm)	% reaction	k
0	0	0	—	0	0	—
0.5	0.94	3.0	0.0257	1.02	5.8	0.0522
1	1.93	6.2	0.0274	2.07	11.6	0.0538
1.5	2.90	9.2	0.0276	3.09	17.3	0.0553
2	3.76	12.0	0.0275	4.08	23.0	0.0569
2.5	—	—	—	4.97	28.1	0.0572
3	5.50	17.5	0.0276	5.83	32.9	0.0577
4	7.19	22.9	0.0285	7.35	41.5	0.0582
5	8.89	28.3	0.0289	8.63	48.7	0.0580
6	10.30	32.7	0.0286	9.73	54.8	0.0576
7	11.69	37.2	0.0288	10.73	60.5	0.0576
10	15.14	48.2	0.0286			
14	19.00	60.5	0.0288			

The effect of surface

In Table III rates are given for an empty reaction vessel, and also for a similar vessel packed with short lengths of Pyrex tubing so as to increase the surface-volume ratio to about 9 times its former value. It will be seen that there is very little difference in the rate in the two vessels. It may therefore be concluded that if any heterogeneous reaction occurs in the empty bulb, it constitutes less than one percent of the whole process.

TABLE III. *The rate of reaction.*

Reaction vessel	Temperature, (°C)	Initial pressure (cm)	$T_{12.5}$ (sec.)	T_{25} (sec.)	T_{50} (sec.)	Reaction vessel	Temperature (°C)	Initial pressure (cm)	$T_{12.5}$ (sec.)	T_{25} (sec.)	T_{50} (sec.)
Empty	189.9	32.68	828	1806	4578	Empty	219.9	33.36	66.0	152	387
"	189.9	36.84	846	1806	4518	"	219.9	37.24	70.8	137	338
"	189.9	mean values	837	1806	4548	"	219.9	44.45	68.4	145	369
"	199.9	20.74	378	798	1908	"	219.9	46.88	67.2	142	360
"	199.9	23.89	348	762	1836	"	219.9	54.50	66.0	142	—
"	199.9	32.95	328	716	1806	"	219.9	mean values	69.3	146.7	378.0
"	199.9	mean values	352	759	1850	"	230.2	14.44	—	61.8	154
"	209.8	13.48	156	323	846	"	230.2	23.21	—	64.2	169
"	209.8	21.14	146	326	834	"	230.2	27.48	—	67.2	174
"	209.8	25.17	141	307	744	"	230.2	30.02	—	63.6	161
"	209.8	26.14	147	315	792	"	230.2	37.48	—	58.8	157
"	209.8	36.57	150	310	792	"	230.2	38.16	—	57.6	152
"	209.8	mean values	148.1	316.2	802	"	230.2	mean values	—	63.3	166.0
"	219.9	5.46	72.0	157	432	"	240.7	18.72	—	29.4	82.2
"	219.9	10.26	72.0	154	369	"	240.7	27.96	—	30.6	81.6
"	219.9	13.02	70.8	134	371	"	240.7	mean values	—	30.0	81.9
"	219.9	13.24	67.8	144	387	Packed	209.8	23.93	136	280	786
"	219.9	20.62	75.0	157	395	"	209.8	29.78	126	267	780
"	219.9	26.34	73.8	154	384	"	219.9	23.35	64.2	145	366
"	219.9	28.40	67.8	144	364	"	219.9	27.72	66.6	144	382
"	219.9	32.87	66.0	132	360	"	230.2	22.85	—	61.8	164
"	219.9	33.29	67.8	148	379	"	230.2	33.38	—	66.6	168

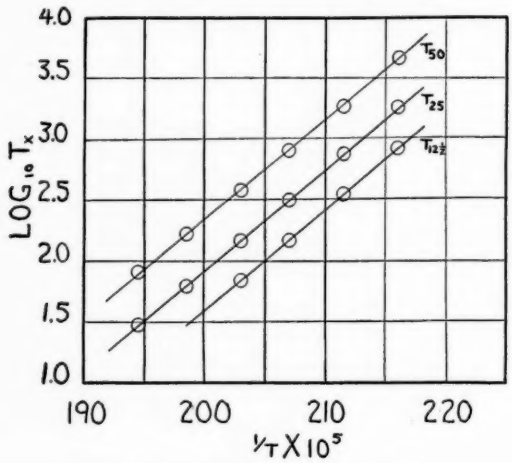

FIG. 1. The temperature coefficient.

The temperature coefficient

In Fig. 1 the logarithms of the fractional times are plotted against the reciprocal of the absolute temperature. The data used are the mean values given in Table III. From the slopes of the lines we obtain the following values for the heat of activation:

From $T_{12.5}$	38,100 calories per gram molecule
From T_{25}	37,550
From T_{50}	37,550
Mean	37,700

The rate of reaction may therefore be expressed by

$$T_{25} = 2.47 \times 10^{-15} e^{37,700/RT} \text{ sec.}$$

Or, since T_{25} represents 29.1 percent reaction,

$$k = 1.39 \times 10^{14} e^{-37,700/RT} \text{ sec.}^{-1}.$$

DISCUSSION

The comparison of the decomposition of ethyl and methyl nitrites is of some interest. Both reactions are extremely simple unimolecular changes in that they presumably involve the direct splitting of only one bond, i.e.,

$$CH_3-O-NO = CH_3O + NO$$

$$C_2H_5-O-NO = C_2H_5O + NO.$$

The activation energies for both reactions are about 37,000 calories. The energy available to break the bond is therefore (37,700 cal. + average energy of the molecules). The number of degrees of freedom involved is at least 12, and is probably much greater. If we assume $n = 12$ and $n = 20$, then we have available at 500°K, 43,000 and 47,000 calories, respectively. There are no direct estimates available of the energy required to split the $-O-NO$ bond. Rice and Johnston[5] found approximately 80,000 calories for C–O, 70,000 to 80,000 for C–C, and about 50,000 for C–N. It therefore seems probable that the energy available here is sufficient to break the O–NO bond. Hence if the reaction in this case proceeds through a free radical mechanism[6] it is not necessary to assume the existence of reaction chains.

The discussion of the effect of chemical configuration on the activation energy, etc., will be deferred until data are available for the propyl and butyl nitrites.

[5] Rice and Johnston, J. A. C. S. **56**, 214 (1934).
[6] Rice and Herzfeld, J. A. C. S. **56**, 284 (1934).

LETTERS TO THE EDITOR

This section will accept reports of new work, provided these are terse and contain few figures, and especially few halftone cuts. The Editorial Board will not hold itself responsible for opinions expressed by the correspondents. Contributions to this section must reach the office of the Managing Editor not later than the 15th of the month preceding that of the issue in which the letter is to appear. No proof will be sent to the authors. The usual publication charge ($3.00 per page) will not be made and no reprints will be furnished free.

Reduction of Oxygen to Hydrogen Peroxide by the Irradiation of Its Aqueous Solution with X-Rays

Irradiation, with x-rays, of oxygen dissolved in water causes its reduction to hydrogen peroxide, because of a primary activation of the water. The amount produced is independent of the oxygen pressure, up to 70 cm. It depends on the hydrogen ion concentration of the solution, as shown by Fig. 1, in which microequivalents of hydrogen peroxide produced per kiloroentgen of dosage are given as a function of the hydrogen ion concentration. The curve is represented by the equation

$$\frac{H_2O_2}{\text{kiloroentgen}} = 2.2\,\frac{1+2\cdot 10^{10.1[\overset{+}{H}]}}{1+10^{10.1[\overset{+}{H}]}}\,\frac{\text{microequivalents}}{1000\text{ cc.}}.$$

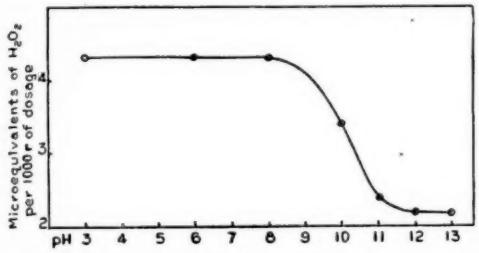

FIG. 1. The production of hydrogen peroxide as a function of the hydrogen ion concentration.

Twice as much hydrogen peroxide is produced in acid as in basic solution. Possibly both atoms of the oxygen molecule are transformed in the former case, as against only one transformed in the latter.

I am indebted to Dr. E. R. Brownscombe for assisting me with these measurements.

HUGO FRICKE
The Dr. Walter B. James Laboratory for Biophysics,
Biological Laboratory,
Cold Spring Harbor, L. I., New York,
April 19, 1934.

Raman Effect in Diiodoacetylene

We are interested in this laboratory in a systematic study of the acetylene bond as affected by substitution of hydrogen by various other elements or radicals. To this end we hope to investigate substituted acetylenes wherein the substituting group is of varying chemical character. Monomethyl acetylene[1] has been reported and the present communication deals with diiodoacetylene. The Raman spectrum of its solutions in alcohol has been studied and five lines have been measured. The frequency shifts of these lines are given in Table I and are believed to represent the fundamental vibrational frequencies of the C_2I_2 molecule. The diiodoacetylene was prepared and purified by the method of Dehn.[2] By using a mercury discharge tube and a filter of 12 mm of a saturated sodium nitrite solution[3] excitation was obtained only from the mercury line of wave-length 4358A. Photographs were taken on a Steinheil spectrograph equipped with glass prisms. The frequency shift corresponding to the C−I vibration (627 cm^{-1}) is about 100 cm^{-1} greater than those observed in iodine compounds of the saturated hydrocarbons.[4] The C⋮C frequency (2109 cm^{-1}) is in the region characteristic of acetylenic compounds and does not support the acetylidine structure of this substance.

TABLE I.

Frequency (cm^{-1})	191	310	627	688	2109
Intensity	strong	medium	weak	weak	strong

Other lines found on the photographic plates could be ascribed to the solvent. The details of this study will be published later.

GEORGE GLOCKLER
CHARLES MORRELL
University of Minnesota,
Minneapolis, Minnesota,
April 19, 1934.

[1] G. Glockler and H. M. Davis, Phys. Rev. **41**, 370 (1932).
[2] W. Dehn, J. Am. Chem. Soc. **33**, 1598 (1911).
[3] H. Pfund, Phys. Rev. **42**, 581 (1932).
[4] A. Dadieu and K. W. F. Kohlrausch, Wien. Ber. **137**, 717 (1930).

Dimensional Relations in the Theory of Electrolytes. A Correction

Recent analyses by Onsager[1] and by Halpern[2] throw considerable light on the foundations of the theory of electrolytes. Much of the previous work is superseded or stands in need of revision. Halpern[2] has called attention to an inconsistency in our treatment of dimensional relations.[3] It can be corrected as follows: From Eq. (10) of our paper and from the relation

$$\partial W/\partial \epsilon_i = \psi_i \tag{1.1}$$

we obtain two values of the second derivative $\partial^2 W/\partial V \cdot \partial \epsilon_i$, which when equated give

$$\psi_i = -\sum_{j=1}^{j=N} \epsilon_j \cdot \frac{\partial \psi_i}{\partial \epsilon_j} - 6V \cdot \frac{\partial \psi_i}{\partial V} \tag{2.1}$$

instead of (14).

In the same way Eqs. (21) and (1.1) lead to

$$\psi_i\left[1-\frac{T}{D}\cdot\frac{dD}{dT}\right]=\left[1+\frac{T}{D}\cdot\frac{dD}{dT}\right]\cdot\sum_{j=1}^{j=N}\epsilon_j\cdot\frac{\partial\psi_i}{\partial\epsilon_j}+2T\cdot\frac{\partial\psi_i}{\partial T} \tag{3.1}$$

instead of (25).

Integrating we obtain:

$$\psi_i = V^{-1/6} \cdot f_1(\epsilon_j / V^{1/6}), \tag{4.1}$$

f_1 being a function of the N arguments $\epsilon_j/V^{1/6}$ and

$$\psi_i = T^{1/2} \cdot D^{-1/2} \cdot f_2(\epsilon_j / T^{1/2} D^{1/2}), \tag{5.1}$$

f_2 being a function of the N arguments $\epsilon_j/T^{1/2}D^{1/2}$.

(4.1) and (5.1) when combined give:

$$\psi_i = V^{-1/6} T^{1/2} D^{-1/2} \cdot f_3(\epsilon_j / V^{1/6} T^{1/2} D^{1/2}). \tag{6.1}$$

Assuming, as is implied in the Debye-Hückel procedure[1] that

$$\psi_1/\epsilon_1 = \psi_2/\epsilon_2 = \cdots = \psi_i/\epsilon_i = \cdots \tag{7.1}$$

and introducing the Boltzmann constant k, (6.1) becomes

$$\psi_i = (\epsilon_i / V^{1/3} D) \cdot f_4(\epsilon_j / (DkT)^{1/2} V^{1/6}). \tag{8.1}$$

It will easily be seen that the Debye-Hückel expression for ψ_i verifies this dimensional relation. Considerations concerning the dependence of ψ_i on the numbers N_j, the ionic strength, etc., could be developed in a manner similar to Halpern's treatment.

PIERRE VAN RYSSELBERGHE

Chemistry Department,
Stanford University,
April 26, 1934.

---

[1] L. Onsager, Chem. Rev. **13**, 73 (1933).

[2] O. Halpern, J. Chem. Phys. **2**, 85 (1934).

[3] P. Van Rysselberghe, J. Chem. Phys. **1**, 205 (1933).